Citation: Bolton, C.T., Stoll, H.M. & Mendez-Vicente, A. (2012), Vital effects in coccolith calcite: Cenozoic climate-pCO2 drove the diversity of carbon acquisition strategies in coccolithophores? PALEOCEANOGRAPHY, VOL. 27, PA4204, doi:10.1029/2012PA002339, 2012

Vital effects in coccolith calcite: Cenozoic climate-pCO_2 drove the diversity of carbon acquisition strategies in coccolithophores?

Clara T. Bolton[1*], Heather M. Stoll[1], Ana Mendez-Vicente[1]

1. Geology Department, University of Oviedo, Arias de Velasco s/n, 33005, Oviedo, Asturias, Spain

*corresponding author, email: cbolton@geol.uniovi.es

Running title: Cenozoic coccolith vital effects

Main point 1: No coccolith stable isotope vital effects during PETM in well preserved site

Main point 2: Clear >1.5‰ range of coccolith vital effects since at least 3.5 Ma

Main point 3: Trend between cell size and C and O isotopic enrichment during Plio-Pleistocene

Abstract

Coccoliths, calcite plates produced by the marine phytoplankton coccolithophores, have previously shown a large array of carbon and oxygen stable isotope fractionations (termed “vital effects”), correlated to cell size and hypothesized to reflect the varying importance of active carbon acquisition strategies. Culture studies show a reduced range of vital effects between large and small coccolithophores under high CO_2, consistent with previous observations of a smaller range of interspecific vital effects in Paleocene coccoliths. We present new fossil data examining coccolithophore vital effects over three key Cenozoic intervals reflecting changing climate and atmospheric partial pressure of CO_2 (pCO_2). Oxygen and carbon stable isotopes of size-separated coccolith fractions dominated by different species from well preserved Paleocene-Eocene thermal maximum (PETM, ~56 Ma) samples show reduced interspecific differences within the greenhouse boundary conditions of the PETM. Conversely, isotope data from the Plio-Pleistocene transition (PPT; 3.5-2 Ma) and the last glacial maximum (LGM; ~22 ka) show persistent vital effects of ~2‰. PPT and LGM data show a clear positive trend between coccolith (cell) size and isotopic enrichment in coccolith carbonate, as seen in laboratory cultures. On geological timescales, the degree of expression of vital effects in coccoliths appears to be insensitive to pCO_2 changes over the range ~350 ppm (Pliocene) to ~180 ppm (LGM). The modern array of coccolith vital effects arose after the PETM but before the late Pliocene and may reflect the operation of more diverse carbon acquisition strategies in coccolithophores in response to decreasing Cenozoic pCO_2.

1. Introduction

Coccolithophorids, unicellular haptophyte algae, play an important role in ocean biogeochemistry because they utilise dissolved inorganic carbon (DIC) in surface waters for both photosynthesis (the 'soft tissue carbon pump') and calcification, producing coccoliths (the 'inorganic carbon pump'). Coccoliths are precipitated intracellularly then extruded through the cell membrane, creating a characteristic carbonate external covering that is preserved in marine sediments [*Pienaar*, 1994; *Brownlee and Taylor*, 2004]. The dual role of coccolithophores in the marine carbon cycle, their long geological history (~225 Ma to present [*Janofske*, 1992; *Bown*, 1998; *Bown et al.*, 2004]) and rapid evolutionary turnover [*Falkowski et al.*, 2004] make this extant phytoplankton group ideal for investigating biotic responses to past, present and projected carbon cycle perturbations through geochemical studies.

Biomineralization in many calcareous marine organisms produces calcite that is not in isotopic equilibrium with ambient seawater [e.g., *Duplessy et al*., 1970; *Weber and Woodhead*, 1972; *Shackleton et al*., 1973; *Anderson and Cole*, 1975; *Margolis et al.*, 1975; *Erez*, 1978; *Grossman*, 1987; *Spero*, 1998; *Steinmetz*, 1994; *Weiner and Dove*, 2003; *Zeebe et al*., 2008]. This variable net isotopic fractionation, historically termed "vital effect" [*Weber and Woodhead*, 1972] because the precise array of equilibrium and kinetic factors causing it remains unknown [e.g., *Erez*, 1978; *Steinmetz*, 1994; *Weiner and Dove*, 2003; *Ziveri et al.*, 2003; *Stoll and Ziveri*, 2004], is of especially large magnitude in coccoliths. In laboratory culture experiments at identical temperature and media composition, coccoliths from different species exhibit a maximum 5‰ range in oxygen and carbon isotopic ratios (measured as ‰ deviation from a standard, $\delta^{18}O$ and $\delta^{13}C$ respectively) [*Dudley and Goodney*, 1979; *Dudley et*

al., 1980; *Dudley et al.*, 1986; *Ziveri et al.*, 2003]. Both $\delta^{18}O$ and $\delta^{13}C$ in coccoliths increase with decreasing cell size in cultured coccolithophores (Fig. 1A, B) [*Ziveri et al.*, 2003; *Rickaby et al.*, 2010] and in natural populations [*Stoll et al.*, 2007a]. No consistent relationship between vital effects and growth rate or phylogeny was observed [*Ziveri et al.*, 2003; *Rickaby et al.*, 2010; *Moolna and Rickaby*, 2012], and the size dependence of isotopic fractionation in coccolith calcite may reflect different carbon acquisition strategies and efficiencies among different-sized species [*Ziveri et al.*, 2003].

Modern algal cells are known to use various carbon concentrating mechanisms (CCMs) to elevate CO_2 in the chloroplast and increase photosynthetic rate [reviewed by *Giordano et al.*, 2005; *Reinfelder*, 2011] . CCMs include active HCO_3^- and CO_2 uptake, or enhancement of diffusive CO_2 uptake with extracellular excretion of the enzyme carbonic anhydrase (CA) to catalyse the conversion between HCO_3^- and CO_2 [e.g., *Raven and Johnston*, 1991; *Badger et al.*, 1998; *Tortell*, 2000; *Rost et al.*, 2003]. Culture experiments with the coccolithophore *Emiliania huxleyi* indicate that photosynthesis is not dependent on calcification as a CO_2 source (i.e., a CCM) under nutrient and light-replete conditions [*Leonardos et al*., 2009]; however cells may use calcification as an energetically cheap way to generate CO_2 for photosynthesis under nutrient or light limitation [*Reinfelder*, 2011; *Schulz et al*., 2007; *Sciandra et al*., 2003]. The need for efficient CCMs is greatest (1) in large cells because they have a smaller surface area to volume ratio, therefore lower diffusive CO_2 transport rates into the cell relative to carbon demand, and (2) at low CO_2 concentrations which limit diffusive CO_2 supply; as has been confirmed by numerous laboratory studies in diverse marine alga [e.g., *Giordano et al.*, 2005; *Falkowski and Raven*, 2007; *Moolna*

and Rickaby, 2012; *Reinfelder*, 2011]. We therefore hypothesize, following previous work [*Stoll*, 2005], that during high pCO_2 intervals CCM significance diminishes, possibly translating into a reduced range of stable isotope signatures among different sized coccoliths. In a recent study, the difference in coccolith $\delta^{18}O$ and $\delta^{13}C$ between a large-celled and a small-celled coccolithophore was reduced at higher culture $CO_{2(aq)}$ [*Rickaby et al.*, 2010] (Fig. 1B).

Long-term reduction in pCO_2 over the Cenozoic (65.5 to 0 Ma) [*Pagani et al.*, 2005; *Royer*, 2006; *Zachos et al.*, 2008] may have forced the evolution of adaptive strategies in phytoplankton. A much smaller range of $\delta^{18}O$ and $\delta^{13}C$ among large and small coccoliths was observed during the Paleocene-Eocene thermal maximum (PETM, ~56 Ma) and could reflect more uniform carbon acquisition strategies at higher ambient pCO_2 [*Stoll*, 2005]. Falling pCO_2 since the early Oligocene may have exerted evolutionary pressure toward a reduction in coccolithophore cell size within some genera [*Henderiks and Pagani*, 2008]. In addition, an observed global decrease in mean assemblage coccolith size over the Cenozoic could result from evolution, abundance and extinction patterns of different-sized species [*Herrmann and Thierstein*, 2012]. To explore coccolith stable isotopic fractionation responses to changing pCO_2 in the past, we present new stable isotope and productivity records of size-separated fossil coccoliths from (1) a new site of latest Paleocene age, (2) the Plio-Pleistocene climate transition (PPT, 3.5 to 2 Ma), and (3) the last glacial maximum (LGM, ~22 ka). For the latest Paleocene, we seek to verify the previous inference that reduced interspecific isotopic differences at Ocean Drilling Program (ODP) Site 690 [*Stoll*, 2005] were not biased by diagenetic homogenisation and/or large coccolithophore assemblage changes by presenting new coccolith geochemical

records from Bass River, New Jersey. We also examine in detail the PPT, which marks the end of long-term cooling culminating in major northern hemisphere glaciation (NHG) [e.g., *Shackleton et al.*, 1984; *Kleiven et al.*, 2002; *Lawrence et al.*, 2009] and encompasses the last major secular pCO_2 decline in Earth's history (~420 to 280 ppm pCO_2 decrease estimated from proxies; Fig. 2) [*Raymo et al.*, 1996; *Pagani et al.*, 2009; *Seki et al.*, 2010; *Bartoli et al.*, 2011]. Our new records show clear, significant (>1.5‰) interspecific vital effects during the PPT and LGM and confirm only minimal differences during the PETM.

2. Materials and Methods

2.1 Samples and site selection

We analysed sediments deposited at Bass River (BR), New Jersey, during the PETM (ODP Site 174AX, 39°36'N, 74°26´W) [*Miller et al.*, 1998] to test whether the absence of significant interspecific isotopic differences reported for PETM-aged coccoliths from Site 690 [*Stoll*, 2005] is a robust environmental signal. Sampling was between 352m and 373m depth at 10-20cm resolution spanning the onset of the PETM negative carbon isotope excursion (CIE) and at 50-200cm resolution before and during the CIE. Sedimentation rates during the PETM were rapid (~10cm/kyr [*Röhl et al.*, 2007]) and silty claystones deposited in a shallow-shelf environment (well above the carbonate lysocline) dominate Paleogene sediments [*Miller et al.*, 2004; *John et al.*, 2008]. The high clay content of these sediments minimises carbonate dissolution that is intrinsic to deep-ocean PETM sections [*Zachos et al.*, 2005], making BR an ideal record to test the findings of *Stoll* [2005].

To investigate coccolithophore vital effects under lower pCO_2 conditions, we analysed PPT and LGM sediments deposited at ODP Site 999 in the Caribbean Sea (12°44'N, 78°44'W; 2830m water depth). Sedimentation at Site 999 is predominantly pelagic with minor aeolian inputs. Plio-Pleistocene sediments constitute clayey Foraminifera and nannofossil ooze with variable carbonate content (40-70%) [*Shipboard Scientific Party,* 1997]. We analysed 22 samples from Site 999A spanning 110.85 to 69.27 metres corrected depth. An orbital-resolution age model was generated via manual correlation of Site 999 benthic foraminiferal $\delta^{18}O$ [*Haug and Tiedemann,* 1998] to the LR04 benthic $\delta^{18}O$ stack [*Lisiecki and Raymo,* 2005] using Analyseries [*Paillard et al.,* 1996]; yielding sedimentation rates of ~2.4-3.6 cm/kyr during our study interval, ~3.5 to 2 Ma. To capture long-term trends in coccolith geochemistry and to minimise variability arising from glacial-interglacial pCO_2 and climate oscillations, which also induce primary productivity fluctuations [e.g., *Bolton et al.*, 2010b], samples were selected from peak interglacials (IG). Samples span marine isotope stages MG7 to 79, with one sample from every or every other IG, depending on sedimentation rate. In the modern ocean, surface waters overlying Site 999 are close to equilibrium with the atmosphere with respect to CO_2 [*Takahashi et al.*, 2009], a scenario that probably prevailed throughout the last glacial cycle [*Foster,* 2008]. Our surface mixed-layer signal will therefore be dominated by large-scale changes in pCO_2 rather than local variations caused by, for example, changes in vertical water-column mixing. To compare our PPT record with data measured on coccoliths deposited under more recent minimum pCO_2 conditions, we analysed LGM sediments from the same site (ODP 999A 1H 1W 100-101cm; ~22 ka age [*Schmidt et al.*, 2004]).

2.2 Coccolith size separations

Bulk sediment samples were gently disaggregated for 24h on a 'ferris wheel' rotating carousel (designer: Nick McCave, pers. comm., 2000), then sieved through a 20µm mesh. A split of the <20µm fraction was used for coccolith size separations, with all steps performed in 2% ammonia solution. Sample-specific repeat decanting protocols following *Paull and Thierstein* [1987] and *Stoll and Ziveri* [2002] were developed to most efficiently separate the species present by size using differences in settling velocities (Fig. 3). A high number of repeats of each step ensured greater separation efficiency. The use of material remaining in suspension rather than settled material reduced contamination by large coccoliths in the smaller size fractions, where a few large coccoliths can skew carbonate contributions to a high degree. For each repeat, the supernatant was carefully removed by plastic syringe, filtered onto a 0.45µm nitrate cellulose filter and resuspended in 2% ammonia. Samples were rinsed 3 times in ultrapure MilliQ water and oven dried at 50°C for several days.

The high species diversity and low carbonate content of BR sediments meant that we focused on obtaining size-restricted (rather than monogeneric) coccolith size fractions (Table 1). A long settling step was first applied to remove fragments <1.5µm. The size fractions 1.5-5µm, 5-8µm and 8-20µm were obtained via settling and subsequent microfiltration (at 8µm) of the settled material. At Site 999, a similar coccolith size distribution during the LGM and the PPT allowed us to use an identical separation protocol for all samples (Fig. 3, Table 2). In PPT samples, we evaluated the effect of contamination by Foraminifera fragments on the isotopic signature of the larger coccolith size fractions (9-12µm and to a lesser extent 6-9µm), by determining $\delta^{18}O$ and $\delta^{13}C$ of the 20-63µm fraction.

2.3 Microscope counts and percent carbonate

All calcareous nannofossil counts were performed on smear slides on a light microscope (LM) under cross-polarized light at x1250 magnification, following the taxonomy of *Perch-Nielsen* [1985] and *Young* [1998]. Hereafter, coccoliths belonging to the Noelaerhabdaceae family (Plio-Plesistocene genera *Reticulofenestra, Pseudoemiliania, Gephyrocapsa* and *Emiliania*) are collectively termed 'reticulofenestrid coccoliths' owing to their similar coccolith structure to *Reticulofenestra* [*Young,* 1998]. A minimum of 400 coccoliths from at least 10 fields of view were counted (>600 coccoliths in PPT <20μm samples because of the dominance of *Florisphaera profunda* and reticulofenestrid coccoliths). Using relative abundances, mean coccolith lengths (determined by LM) and shape constants (k_s values) [*Young and Ziveri* 2000], coccolith volume and carbonate contributions were calculated. Where a k_s value for the exact species or genus was unavailable, the closest species was used (e.g. *Gephyrocapsa oceanica* for *Reticulofenestra*). Although cumulative errors in these calculations are typically large [*Young and Ziveri*, 2000], carbonate contribution data give a much clearer idea of the origin of the isotopic signals contained in a mixed-species sample than relative abundance data, where equal weight is given to all coccoliths regardless of size or shape.

For the PETM samples, whole-assemblage calcareous nannofossil abundance data were available [*Gibbs et al.*, 2010; *S. J. Gibbs, pers. comm.*], thus counts were performed on the three size fractions of six samples covering the interval of maximum change in assemblage and bulk carbonate isotope composition (356.95m to 357.90m). Abundances were converted to carbonate contributions as described above (Supp. Fig.

1B, Table 1). For all PPT samples, counts were performed on the <20µm fraction to determine bulk assemblage composition (Supp. Fig. 2A). Relative abundances of *F. profunda* and very small *Reticulofenestra* sp. (VSR, <3µm), two groups with similar dissolution susceptibilities [*Gibbs et al.*, 2004], were used in the *N ratio* (N=VSR/VSR+Fp) as an indicator of coccolithophore productivity [*Beaufort et al.*, 1997; *Flores et al.*, 2000; *Bolton et al.*, 2010a]. To obtain a reliable approximation of species carbonate contribution in each size fraction throughout the time series, counts were performed on all five size fractions for PPT samples 2 (2180 ka), 9 (2660 ka) and 21 (3392 ka) and the LGM sample (Table 2). For the two smallest size fractions, essentially constituting mixtures of only small reticulofenestrid (<4µm) and *F. profunda* coccoliths, end member isotopes were calculated using carbonate contributions (for the PPT, mean values of the counted samples were used, Table 2).

2.4 Stable isotope analysis

Stable isotope ratios on BR samples were measured at Woods Hole Oceanographic Institute on a Finnegan MAT 253 dual-inlet isotope ratio mass spectrometer (DI-IRMS) with a Kiel III Carb Device with analytical precision of 0.08‰ for $\delta^{18}O$ and 0.03‰ for $\delta^{13}C$ (1σ). A higher-resolution sample set between 358.81m and 356.95m was later run at the University of California Santa Cruz on a GVI Prism DI-IRMS with an analytical precision of 0.08‰ for $\delta^{18}O$ and 0.05‰ for $\delta^{13}C$. Different size fractions from the same sample were always analysed together, thus potential interlab offsets cannot affect inter-fraction isotopic differences. PPT and LGM stable isotope data were generated on a Nu Instruments Perspective DI-IRMS connected to a NuCarb carbonate preparation system at the University of Oviedo with analytical precision of 0.06‰ for $\delta^{18}O$ and 0.05‰ for $\delta^{13}C$ (1σ). Duplicate analyses show mean

reproducibility of 0.07‰ ($\delta^{18}O$) and 0.05‰ ($\delta^{13}C$) (1σ). 1mg splits of PPT 20-63µm fractions were analysed on a Nu Instruments Horizon continuous flow (CF)-IRMS connected to a gas preparation system at the University of Oviedo with analytical precision of 0.1‰ for $\delta^{18}O$ and 0.08‰ for $\delta^{13}C$ (1σ). All stable isotopes are reported relative to the Vienna Pee Dee Belemnite (VPDB) standard.

2.5 Strontium/Calcium

Sr/Ca in coccoliths was measured to define productivity (growth rate) variations that could affect interpretation of temporal or interspecific trends in stable isotope data. In BR samples (where clays dominate sediments thus reliable data cannot be obtained from bulk sediment analysis) Sr/Ca was measured by ion probe analysis on monospecific populations of 12-20 individually picked coccoliths (see *Stoll et al.* [2007b] and *Stoll and Shimizu* [2009] for methods). Populations of small and medium *Toweius* sp. and *Coccolithus pelagicus* coccoliths were measured. A subset of the medium *Toweius* Sr/Ca data appears in *Gibbs et al.* [2010].

In PPT samples, Sr/Ca was measured in the small reticulofenestrid (2.5-4µm) and large *Helicosphaera* (6-9µm) coccolith size fractions. Subsamples were cleaned with reducing and ion exchange treatments (see *Stoll and Ziveri* [2002]) then gently dissolved in acetic acid with an ammonium acetate buffer for 12h. Calcium content was analysed on splits of all samples, which were then diluted to constant calcium concentrations for Sr/Ca analysis by inductively coupled plasma optical emission spectroscopy (ICP-OES) on a Thermo ICAP DUO 6300 at the University of Oviedo. Although Sr/Ca in coccoliths varies with growth rate, there is also a known temperature influence [*Stoll and Schrag*, 2000; *Rickaby and Schrag*, 2002; *Stoll et al.*,

2002; 2007c]. To isolate the productivity component, variance attributable to sea surface temperature (SST) was subtracted from Sr/Ca. We used the *Globigerinoides sacculifer* Mg/Ca-derived SST record for Site 999 [*Groeneveld*, 2005], resampled and interpolated to the same depths as our samples, and Sr/Ca-temperature relationships derived for *Gephyrocapsa oceanica* and *Helicosphaera carteri* [*Stoll et al.*, 2002].

3. Results

3.1 Coccolith separation efficiency

In BR samples, size-separation efficiency was excellent for medium-sized coccoliths (5-8µm) and modest for small-sized coccoliths (1.5-5µm). The reduction in efficiency observed for small coccoliths occurred because a minor percentage of medium-sized liths (<10% rel. abundance) make a disproportionately large mass contribution to this size fraction (e.g., a 5µm lith weighs 57pg versus 7pg for a 2.7µm lith). The BR 8-20µm fraction was dominated (>50% carbonate mass) by Foraminifera fragments therefore was not used further in this study (Table 1, Supp. Fig. 1B). The small coccolith fraction (1.5-5µm) predominantly contains small Prinsiaceae coccoliths, mainly *Toweius* species. A large influx of small (<3µm) placoliths at the CIE onset alters the relative contribution of small versus larger coccoliths. However, mutual relative abundances of medium and large placoliths (*Coccolithus pelagicus*, *Toweis pertutus*, other *Toweis* sp., and *Prinsius* sp.), the constituents of our 5-8µm coccolith size fraction, remain similar (Supp. Fig. 1A) [*Gibbs et al.*, 2010; *S. J. Gibbs, pers. comm.*]. Thus, our size-restricted BR coccolith fractions have relatively constant species composition despite assemblage changes over the PETM interval.

Separation efficacy of Site 999 coccoliths was very good, resulting in five distinct size-classes. In three of these, carbonate was dominated (65-90%) by a single species or family (Table 2). For the PPT, the <2.5µm fraction is dominated by *F. profunda* coccoliths and the 2.5-4µm fraction by small reticulofenestrid coccoliths (*Reticulofenestra* and to a lesser extent *Pseudoemiliania*). The 4-6µm fraction contains medium-sized coccoliths of mixed species, including larger *Reticulofenestra, Pseudoemiliania, Umbilicosphaera,* and smaller *Helicosphaera* coccoliths. The 6-9µm fraction is dominated by *Helicosphaera* coccoliths, predominantly *H. carteri*. In the 9-12µm fraction, *Helicosphaera* coccoliths dominate in younger samples, with increasing contribution from *Discoaster* nannoliths in older samples. Foraminifera fragments contribute to the 9-12µm fraction throughout, with slightly decreasing abundance downcore. Relatively uniform bulk assemblage composition and size distribution mean that the composition of size fractions is relatively constant from 3.5 to 2 Ma (Table 2; Supp. Fig. 2). LGM size fractions are dominated by the same species or genera as PPT samples, with the following exceptions: the 2.5-4µm fraction is dominated by the genera *Gephyrocapsa* and *Emiliania*, and the 9-12µm fraction is almost entirely composed of dinoflagellate calcispheres of the *Thoracosphaeraceae* family (Table 2). The high efficiency of size separation achieved for coccoliths from the PETM, PPT and LGM allowed us to generate stable isotope data on a large range of narrow size classes, permitting meaningful interpretation of geochemical data in terms of ancient coccolithophore cell size.

3.2 Stable isotopes

PETM coccoliths faithfully record the CIE at BR with a ~3‰ negative shift in $\delta^{18}O$ and $\delta^{13}C$ in both size fractions around 359m, coincident with the CIE onset recorded

in bulk and foraminiferal carbonate and with similar values to those measured in bulk carbonate (Fig. 4A, B). Coccoliths record a similar-sized $\delta^{13}C$ shift as the surface-dwelling Foraminifera *Acarinina* sp. and a larger shift than recorded in the benthic Foraminifera *Cibicidoides* sp. [*John et al.*, 2008]. Critically to this study, coccolith stable isotopes exhibit negligible differences between small (1.5-5µm) and larger (5-8µm) size fractions for $\delta^{13}C$ (mean difference 0.17‰), with smaller coccoliths in most samples showing a slight $\delta^{18}O$ enrichment relative to larger coccoliths (mean difference 0.66‰) (Fig. 4A, B).

We isolate temporal changes in interspecific isotopic differences in our Plio-Pleistocene data by removing the imprint of cooling and ice-sheet expansion associated with NHG; achieved by subtracting the stable isotopic composition of co-existing planktic Foraminifera (*Globigerinoides sacculifer*) from our PPT and LGM coccolith isotope data (Fig. 5; uncorrected data Supp. Fig. 3). Our Plio-Pleistocene coccolith fractions typically exhibit a much greater range of isotopic values compared to our PETM fractions. Data show $\delta^{18}O$ and $\delta^{13}C$ ranges of ~1.5 to 2‰ (PPT) and ~1.3 to 1.5‰ (LGM) between smallest and largest coccolith size fractions, with $\delta^{18}O$ and $\delta^{13}C$ values increasing with decreasing coccolith size (Figs. 5, 6A & E). The $\delta^{18}O$ and $\delta^{13}C$ ranges between fractions do not show long-term temporal trends over the PPT (Figs. 5, 6, and 7C). Two samples around 2.6 Ma contain a reduced array of isotopic values because more negative $\delta^{18}O$ and $\delta^{13}C$ are recorded by the 2.5-4µm fraction (Fig. 5, pink shading in Fig. 7C). LM inspection of this size fraction in all PPT samples indicates an isolated change in species composition, with these two samples containing (1) a greater proportion of *Pseudoemiliania ovata* (~4µm) relative to *Reticulofenestra minuta* (<3µm) coccoliths and (2) more dislocated *Discoaster*

arms than other samples. These factors are both consistent with the more negative isotopic signature recorded; therefore we interpret data in this interval to reflect a change in carbonate source for some size fractions rather than a contraction of interspecific differences. The 20-63µm fraction records more positive $\delta^{18}O$ and $\delta^{13}C$ than the two largest coccolith fractions (Figs. 5, 6), thus the presence of Foraminifera fragments in these fractions potentially reduces the measured range of isotopic values between small and large coccoliths. Increasing foraminiferal fragment abundance upcore could also mask an increase in the isotopic array between different sized coccoliths driven by more depleted values in the large coccoliths.

We plot PPT coccolith isotopes with Site 999 Foraminifera isotopes to illustrate the distinct trends in the two calcifier groups (Fig. 8, see caption for details). Foraminifera record an inverse correlation between $\delta^{18}O$ and $\delta^{13}C$, whereas coccoliths record a positive $\delta^{18}O$-$\delta^{13}C$ correlation. The $\delta^{18}O$ signature of the 20-63µm fraction is consistent with a mixed-species planktic Foraminifera origin; however the depleted $\delta^{13}C$ in this size fraction suggests additional contribution from large coccoliths (confirmed by LM; samples were not ultrasonicated to remove adhering coccoliths and sieving at 20µm can be inefficient given the small open area of the mesh). In Figure 9, we illustrate BR coccolith and Foraminifera isotopes as mean values (see caption for details). Like at Site 999, Foraminifera display an inverse $\delta^{18}O$- $\delta^{13}C$ correlation. Conversely, small versus larger coccolith size-fractions show very similar $\delta^{13}C$ values and a $\delta^{18}O$ range of <0.75‰. As expected due to the dominance of coccolith carbonate, bulk sediment records a mean isotopic signature closer to that of coccoliths than Foraminifera (Fig. 9).

3.3 Productivity

PETM coccolith Sr/Ca ranges between 1.8 and 2.8 mmol/mol. Before and after the CIE onset interval (~355-359m), coccolith Sr/Ca is variable and high values (elevated productivity) coincide with low sea level as inferred from dinoflagellate cyst assemblages (Spiniferites to *Areoligera* ratio, S-A ratio) (Fig. 4) [*Sluijs*, 2006]. Where Sr/Ca data exist for small and medium *Toweius* and large *Coccolithus*, similar trends and values are observed, with an initial decrease in Sr/Ca at the CIE onset followed by two peaks then decreasing values (Fig. 4C). During this early PETM interval (355-358m), the relationship between coccolith Sr/Ca and the dinocyst S-A ratio deviates from the previous trend in showing high productivity despite high sea levels (Fig. 4). BR coccolith stable isotopes and Sr/Ca are uncorrelated (R^2 <0.1).

PPT Sr/Ca in the small reticulofenestrid and *Helicosphaera* coccolith fractions varies in the range 2.17-2.53 mmol/mol and 2.09-2.75 mmol/mol respectively, with both timeseries following similar trends but with greater amplitude variability in *Helicosphaera* Sr/Ca (Fig. 7A, dashed lines). Removal of the SST component from Sr/Ca, leaving a residual record attributed to productivity, does not alter the main trends or amplitude variation in the uncorrected Sr/Ca (Fig. 7A, solid lines). Productivity maxima occur at ~400 ka intervals (Fig. 7A). The independent *N ratio* productivity proxy shows similar trends to Sr/Ca productivity records; however maxima and minima are sometimes offset between floral and geochemical records (Fig. 7B). Although certain features in coccolith isotope and productivity records appear coincident (Fig. 7), no significant correlations were found (R^2 <0.2).

4. Discussion

4.1 Are coccolith isotope variations due to depth habitats?

Variations in the $\delta^{13}C$ of DIC, SST, salinity and CO_3^{2-} concentration throughout the photic zone are expected to influence the equilibrium isotopic composition of carbonate formed at different depths. Thus, deeper-dwelling calcifiers record the more positive $\delta^{18}O$ of colder waters and a more negative $\delta^{13}C$ than upper photic zone (UPZ) species because of remineralisation of ^{12}C-enriched organic matter at depth [e.g., *Fairbanks et al.*, 1982; *Rohling et al.*, 2004]. Oceanographic studies found that most coccolithophores inhabit the UPZ (0-100m), with a few specialised species, e.g. *F. profunda* and *Thorosphaera flabellata*, living in the deep photic zone (DPZ, >100m) [*Okada and Honjo*, 1973; *Honjo and Okada*, 1974]. Our *F. profunda* (smallest) coccolith fraction records the heaviest $\delta^{18}O$ of all fractions, as predicted by its deep habitat; however it also records the most positive $\delta^{13}C$, suggesting that depth habitat does not exert primary control on its isotopic composition (Fig 5, Supp. Fig. 3). Furthermore, the interspecific $\delta^{13}C$ range recorded may be reduced as a result of the depth habitat of *F. profunda* relative to UPZ coccolithophores. At Site 999 and BR, trends in coccolith isotopes are distinct from trends predicted by depth habitat, as illustrated by the isotopic signatures of coexisting Foraminifera [*Fairbanks et al.*, 1982; *Rohling et al.*, 2004; *Steph et al.*, 2009] (Fig. 8, 9). Thus, the trend of increasing isotopic enrichment with decreasing coccolith size at Site 999 appears independent of depth habitat.

4.2 Cell size control over variable stable isotopic fractionation since the Pliocene

4.2.1 Processes linking cell size and variable isotopic fractionation

It has long been recognized that many biogenic carbonates have $\delta^{18}O$ and $\delta^{13}C$ signatures that differ from an abiogenic calcite precipitated from the same seawater [e.g., *McConnaughey*, 1989a, b]. In coccolithophores, these non-equilibrium offsets, or vital effects, correlate strongly with cell size in cultures and recent sediments [*Ziveri et al.*, 2003; *Stoll et al.*, 2007a]. In cultures, the magnitude of interspecific vital effects in coccoliths diminishes with increasing CO_2 [*Rickaby et al.*, 2010]. Our interpretation of results from the sediment record is based on these empirical correlations between vital effects, cell size and CO_2 (Fig. 1).

The processes responsible for vital effects have been explored in several organisms and probably vary amongst biogenic carbonate producers. Foraminifera exhibit a strong 'carbonate ion effect' on both carbon and oxygen isotopic composition, resulting in decreased $\delta^{18}O$ and $\delta^{13}C$ with increasing media [CO_3^{2-}] and pH [*Spero et al.*, 1997; *Bijma et al.*, 1999]. *Zeebe* [1999] proposed that as the proportion of isotopically lighter CO_3^{2-} relative to isotopically heavier HCO_3^- increases at higher pH, the $\delta^{18}O$ of total dissolved inorganic carbon (ΣCO_2) decreases. Thus the $\delta^{18}O$ of precipitated $CaCO_3$ will be lighter at higher pH providing calcite is formed from a mixture of the carbonate species in proportion to their relative contribution to ΣCO_2 [*Zeebe*, 1999]. This same mechanism was recently modelled for the coccolithophore *Calcidiscus leptoporus*, whereby a higher ratio of CO_3^{2-} to HCO_3^- delivered to the calcification vesicle results in the formation of $\delta^{18}O$-depleted coccoliths at higher media pH [*Ziveri et al.*, 2012]. For both Foraminifera and coccolithophores, this model is applicable only to $\delta^{18}O$ (not $\delta^{13}C$), because oxygen isotopes reach chemical

equilibrium in the ΣCO_2 system significantly faster than isotopic equilibrium (~16sec vs. ~10h at 25°C, pH 8.2, salinity 35 [*Zeebe et al.*, 1999]). As a single *C. leptoporus* coccolith is formed in ~1.4h [*Ziveri et al*., 2012 calculated from *Langer et al.*, 2006], CO_3^{2-} converted from HCO_3^- within the calcification vesicle will transfer the heavier $\delta^{18}O$ fingerprint of HCO_3^- to the coccolith [*Ziveri et al*., 2012].

Other processes probably also operate in coccolithophores, since culture studies with constant pH but changing ΣCO_2 resulted in a variable degree of carbon and oxygen isotopic fractionation into coccolith calcite [*Rickaby et al.*, 2010]. One hypothesis is that, under high ΣCO_2 culture conditions with constant pH (therefore high $[CO_3^{2-}]$ and $[HCO_3^-]$ but constant HCO_3^-:CO_3^{2-} ratio), the large species *Coccolithus pelagicus ssp. braarudii* utilises more HCO_3^- relative to CO_3^{2-} for calcification compared to under low ΣCO_2, potentially via manipulation of coccolith-vesicle pH [*Rickaby et al*., 2010]. This process is inferred to explain the observed heavier $\delta^{18}O$ and $\delta^{13}C$ of *C. pelagicus ssp. braarudii* coccoliths at high ΣCO_2, one consequence of which is a reduced difference between the $\delta^{13}C$ and $\delta^{18}O$ of coccoliths precipitated by small (*G. oceanica*) versus large (*C. pelagicus ssp. braarudii*) coccolithophores at high ΣCO_2 (Fig. 1B) [*Rickaby et al*., 2010].

The suite of cellular transport and fractionation processes responsible for the correlation between isotopic fractionation in coccolith carbonate and cell size has not yet been quantitatively explored. Cell size is a fundamental control on unicellular algal physiology because it controls rates of diffusive transport of essential dissolved compounds (nutrients, CO_2, waste products) into and out of the cell. Thus, small cells with a lower carbon cell quota (approximated to cell volume) relative to surface area

and a smaller diffusive boundary layer will be able to replenish resources more rapidly, allowing for higher maximum growth rates [*Raven,* 1998] and strongly affecting carbon isotopic fractionation into organic matter [*Popp et al.,* 1998].

4.2.2 Is variable isotopic fractionation in PPT coccoliths correlated to cell size?

Our protocols separate different sized coccoliths that we infer were produced by coccolithophores of different sizes. A detailed study of coccolith, coccosphere, and cell size amongst several placolith-bearing spherical genera in the fossil record (*Reticulofenestra*, *Cyclicargolithus* and *Coccolithus*) indicates strong linear relationships between these parameters, consistent with relationships in modern descendent species [*Henderiks,* 2008]. Thus, we assume that fossil coccolith size is proportional to cell size in related or morphologically similar species (e.g., *Umbilicosphaera sibogae* var. *foliosa* and *Calcidiscus leptoporus* [*Young et al.*, 2004]). In contrast, *F. profunda*, a poorly understood species with a unique morphology, could be an exception to the trend of increasing isotopic enrichment with decreasing cell size. Morphometric analyses indicate that *F. profunda* coccospheres are large relative to coccoliths (7-8µm sphere, 2µm liths [*Quinn et al.*, 2005]) compared to other species (*Reticulofenestra*: ~7µm sphere, 4µm liths [*Henderiks*, 2008]; *Helicosphaera carteri*: ~14µm cell diameter [*Ziveri et al.*, 2003], ~18µm sphere and 8-9µm liths [estimated from *Young et al.* 2004]). We speculate that the heavy isotopic signature recorded in *F. profunda* coccoliths could relate to the low $[CO_3^{2-}]$ and high $[CO_{2(aq)}]$ in this species' deep habitat relative to the shallower habitat of the placoliths. Reduced CO_2 limitation in the DPZ could enable *F. profunda* to meet a greater portion of its carbon quota by CO_2 diffusion. If the magnitude of vital effect is influenced by the relative importance of CCMs to carbon

acquisition, this could explain the similar isotopic signature in *F. profunda* and the smallest-celled UPZ coccoliths. Within the PPT placoliths, cell size, rather than phylogeny, appears to regulate isotopic fractionation. The 4-6µm coccolith size-fraction is a mixture of species from diverse lineages yet isotopically it falls between smaller and larger coccoliths, as expected if cell size were the dominant control (Fig. 6).

4.2.3 Coherency of size-related isotopic fractionation in fossil coccoliths with cultures and sediment traps

$\delta^{18}O$ and $\delta^{13}C$ differences in Plio-Pleistocene fractions dominated by *F. profunda*, small reticulofenestrid and *Helicosphaera* coccoliths (Fig. 5, 6) are of similar magnitude to those measured in sediment trap material from the Bay of Bengal in size fractions dominated by the same three coccolith groups and interpreted as resulting primarily from size-controlled variable isotopic fractionation [*Stoll et al.*, 2007a]. Similarly, our PPT and LGM data show trends consistent with culture studies, although interspecific isotopic differences for a given coccolith size range are greater in culture [*Dudley and Goodney*, 1979; *Dudley et al.*, 1980; *Ziveri et al.*, 2003] than in fossil and trap material [this study; *Stoll et al.*, 2007a]. This could be partly attributable to the distinct conditions in a laboratory culture set-up versus an open ocean environment. In nutrient and light replete culture growth media, experiments might show the maximum possible range of vital effects because light or nutrients do not limit the potential extra energy requirements necessary to operate CCMs. In nature, below-optimal nutrient (e.g., phosphate, nitrate or iron) or light levels are common and may limit the extent of CCM operation [*Gervais and Riebesell*, 2001;

Rost et al., 2003; *Giordano et al*., 2005; *Cassar et al.*, 2006; *Raven el al.* 2008; *Schulz et al.*, 2007].

4.3 To what extent does productivity influence vital effects?

While there has been no systematic evaluation of the effect of productivity on stable isotope vital effects in coccolith calcite, high algal growth rate has been shown to reduce carbon isotopic fractionation into organic matter during photosynthesis, presumably by increasing cellular carbon demand relative to diffusive CO_2 supply [*Bidigare et al.*, 1997]. Estimated phosphorus concentrations are routinely employed to correct for such growth rate effects when inferring fractionation due to changing CO_2 levels [e.g., *Bidigare et al.*, 1997; *Pagani et al.*, 1999; *Seki et al*., 2010]. The significance of active carbon uptake in coccolithophores [e.g. Nimer *et al.*, 1992; Dong et al. 1993; *Rost et al.* 2003; *Cassar et al.*, 2006; *Trimborn et al.*, 2007] to the cell budget is probably conditioned by the balance of diffusive CO_2 availability and cellular carbon demand. At high growth rates, large cells have a greater relative limitation by diffusive CO_2 supply than smaller cells and consequently models predict a greater difference between organic carbon isotopic composition of small and large cells [*Rau et al*., 1996]. In Bay of Bengal sediment traps, coccoliths produced during the high productivity upwelling or eddy-pumping season exhibit a greater difference between the $\delta^{18}O$ and $\delta^{13}C$ of larger and smaller size fractions (*H. carteri* and *C. leptoporus* versus *G. oceanica*) [*Stoll et al*., 2007a]. In cultures with constant carbon chemistry but variable light levels, higher growth rates led to a ~1‰ greater difference between $\delta^{18}O$ in large *C. leptoporus* and small *G. oceanica* coccoliths (Fig. 1C) [*Ziveri et al.*, 2003].

Within a given species, coccolith Sr/Ca may be a useful indicator of the growth rate effects on carbon isotopic fractionation into organic carbon [*Stoll and Schrag*, 2000; *Stoll et al*., 2002]. Therefore we examined whether any significant changes in Sr/Ca occurred during our study intervals that could possibly attenuate or magnify coccolith vital effects during our study intervals. The PPT at Site 999 is likely to have more stable productivity effects than the PETM at Bass River because of the nature of the climate transition and geographical setting (open-ocean oligotrophic versus dynamic shelf environment). Although there is no significant correlation, some peaks in PPT productivity appear to be synchronous with maxima in interspecific coccolith isotope differences (Fig. 7), suggesting some productivity influence on isotopic fractionation into coccoliths.

During the PETM at Bass River, no large changes in the difference between stable isotopic composition of small and medium coccoliths occur. However productivity inferred from coccolith Sr/Ca exhibits clear variability apparently related to sea level fluctuations. Prior to the PETM, intervals of low sea level inferred from dinoflagellate assemblages [*Sluijs et al.*, 2007] are characterized by elevated coccolithophore productivity (Fig. 4). We interpret this to reflect increased proximity to terrestrial nutrient sources and/or increased turbulent mixing in a shallower water column, injecting nutrient-rich deeper waters into the UPZ. The first part of the PETM (356-358m) deviates from this trend in showing high productivity despite high sea levels, suggesting significant enhancement of terrestrial nutrient supply overriding the sea level influence. This interpretation is consistent with evidence for increased river discharge to the New Jersey margin during this time including increased abundance of low salinity dinocysts [*Sluijs et al.*, 2007] and magnetofossil data suggesting a tropical

river system existed on the mid-Atlantic coastal plain of the USA during the PETM [*Kopp et al.*, 2009]. Changes in productivity at BR appear not to affect the magnitude of inter-fraction coccolith $\delta^{18}O$ and $\delta^{13}C$ observed, which remain low throughout the record (Fig. 4).

4.4 Variable expression of coccolith vital effects over the Cenozoic pCO_2 decline

BR data show only small $\delta^{13}C$ and $\delta^{18}O$ differences (mean 0.17‰ and 0.66‰ respectively) between small and medium-sized coccoliths (Fig. 4 & 9) compared to modern interspecific differences (up to 5‰). These new data from very well-preserved coccoliths agree with previous PETM data from ODP Site 690 [*Stoll*, 2005]; confirming that diagenetic homogenisation is not the principal driver of the small differences observed between different-sized Palaeocene coccoliths. The slight $\delta^{18}O$ enrichment observed in the BR smaller coccolith fraction relative to the larger one is inconsistent with a different depth habitat relative to the larger coccoliths (Section 4.1), and may represent a small cell-size related vital effect, given that the mechanisms causing fractionation in $\delta^{18}O$ and $\delta^{13}C$ in coccoliths may be decoupled in some circumstances. The main constituents of the Bass River PETM size-fractions, coccoliths of the genera *Toweius*, *Coccolithus* and *Prinsius* (Supp Fig. 1), are all placoliths likely to conform to lith:cell size relationships detailed in section 4.2.2 [*Henderiks*, 2008]. Therefore the finding that, during the PETM, larger coccolithophores did not consistently produce more isotopically depleted coccoliths as they do during the PPT, LGM, modern ocean and laboratory appears robust, and may be an expression of more uniform carbon acquisition strategies amongst Palaeocene coccolithophores.

CCMs in the Haptophyta may have existed since ~300 Ma [*Young et al*., 2012]. However, their degree of expression and significance to whole-cell carbon acquisition probably changed as a function of $CO_{2(aq)}$, nutrient availability and other factors over the course of the Earth´s history [*Tortell*, 2000], as occurs over a range of CO_2 in laboratory cultures [e.g., *Giordano et al.*, 2005; *Falkowski and Raven*, 2007; *Moolna and Rickaby*, 2012; *Reinfelder*, 2011]. Our data suggest that the array of stable isotope vital effects in fossil coccoliths, potentially one expression of the carbon acquisition strategies employed by ancient cells, is related to past climate and CO_2 concentrations during the Cenozoic. This is consistent with culture studies showing reduced CCM activity and reduced $\delta^{18}O$ and $\delta^{13}C$ differences between small and large coccolithophores with higher ambient carbon availability [*Rickaby et al.*, 2010; *Moolna and Rickaby*, 2012].

5. Summary & conclusions

The data presented here provide two Cenozoic end-members between which the ranges of oxygen and carbon stable isotopic compositions of different-sized coccoliths reached their modern array. New PETM data confirm previously reported reduced interpecific differences in coccolith stable isotopes within ‘greenhouse’ climate boundary conditions at this time, and PPT and LGM coccoliths record persistent 1.5-2‰ vital effects. These temporal trends and the correlation between isotopic fractionation and size in PPT and LGM coccoliths, consistent with culture data, suggest that vital effects may be linked in some way to coccolithophore carbon acquisition strategies and the level of expression of CCMs in response to the changing paleoenvironment (e.g., $CO_{2(aq)}$ concentration, nutrient availability). Coccolith vital effects were insensitive to pCO_2 changes over the range inferred for the PPT (~400 to

280 ppm, corresponding to a change in $CO_{2(aq)}$ of ~10.5 to 6.5 µmol/kg SW at Site 999). During the PPT, productivity fluctuations may have affected isotopic fractionation into coccoliths to a small degree, in the same sense as previously reported for carbon isotopic fractionation into organic matter. During the PETM at BR, stable isotopic differences between size-fractions remain small despite significant changes in productivity that appear correlated to sea level fluctuations on the New Jersey coastal plain. Experimental data on the effect of nutrient and light availability and growth rate on isotopic fractionation into coccoliths in multiple species is currently lacking and would allow for more accurate assessment of potential factors driving coccolith stable isotopes in the fossil record.

6. Acknowledgements

This work used samples provided by the (Integrated) Ocean Drilling Program (IODP). The IODP is sponsored by the US National Science Foundation and participating countries under management of the Joint Oceanographic Institutions (JOI), Inc. We thank Williams College undergraduate research assistants Alicia Jackson and Danielle Zentner for help processing Bass River samples, and Nobu Shimizu of the Woods Hole Northeast National Ion Probe Facility for assistance with Sr/Ca ion probe determinations. We are grateful to John Morrison for expert help during Site 999 stable isotope analyses, Rindy Ostermann for assistance with stable isotope analyses at WHOI and also to staff at Santa Cruz stable isotope laboratory. We thank Ian Bailey and Kirsten Isensee for discussions and comments on an earlier version of the manuscript, Jeroen Groeneveld for access to unpublished data, and reviewers for comments that helped improve the manuscript. All authors acknowledge European Research Council grant UE-09-ERC-2009-STG-240222-PACE, awarded to HMS.

HMS also acknowledges funding from National Science Foundation grant EAR-0628336.

References

Anderson, T. F., and S. A. Cole (1975), The stable isotope geochemistry of marine coccoliths; a preliminary comparison with planktonic Foraminifera, *Journal of Foraminiferal Research*, *5*, 188-192.

Badger, M. R., T. J. Andrews, S. M. Whitney, M. Ludwig, D. C. Yellowlees, W. Leggat, and G. D. Price (1998), The diversity and coevolution of Rubisco, plastids, pyrenoids, and chloroplast-based CO_2-concentrating mechanisms in algae, *Canadian Journal of Botany*, *76*(6), 1052-1071.

Bartoli, G., B. Hönisch, and R. E. Zeebe (2011), Atmospheric CO_2 decline during the Pliocene intensification of Northern Hemisphere glaciations, *Paleoceanography*, *26*, PA4213.

Beaufort, L., Y. Lancelot, P. Camberlin, O. Cayre, E. Vincent, F. Bassinot, and L. Labeyrie (1997), Insolation Cycles as a Major Control of Equatorial Indian Ocean Primary Production: *Science*, *278*, 1451-1454.

Bidigare, R. R., A. Fluegge, K. H. Freeman, K. L. Hanson, J. M. Hayes, D. Hollander, J. P. Jasper, L. L. King, E. A. Laws, J. Milder, F. J. Millero, R. D. Pancost, B. N. Popp, P. A. Steinberg, and S. G. Wakeham (1997), Consistent fractionation of ^{13}C in nature and in the laboratory: Growth rate effects in some haptophyte algae, *Global Biogeochemical Cycles*, *11*(2), 279-292.

Bijma, J., H. J. Spero, and D. W. Lea (1999), Reassessing foraminiferal stable isotope geochemistry: Impact of the oceanic carbonate system (experimental results),

in *Use of Proxies in Paleoceanography: Examples from the South Atlantic*, edited by G. Fischer and G. Wefer, pp. 489-512, Springer-Verlag, New York.

Bolton, C. T., S. J. Gibbs, and P. A. Wilson (2010a), Evolution of nutricline dynamics in the equatorial Pacific during the late Pliocene, *Paleoceanography*, *25*, PA1207.

Bolton, C. T., K. T. Lawrence, S. J. Gibbs, P. A. Wilson, L. C. Cleaveland, and T. D. Herbert (2010b), Glacial–interglacial productivity changes recorded by alkenones and microfossils in late Pliocene eastern equatorial Pacific and Atlantic upwelling zones, *Earth and Planetary Science Letters*, *295*, 401-411.

Bown, P. (1998), *Calcareous nannofossil biostratigraphy*, Chapman & Hall, Cambridge.

Bown, P., J. A. Lees, and J. R. Young (2004), Calcareous nannoplankton evolution and diversity through time, in *Coccolithophores: From molecular processes to global impact*, edited by H. R. Thierstein and J. R. Young, Springer-Verlag, Berlin Heidelberg.

Brownlee, C., and A. Taylor (2004), Calcification in coccolithophores: A cellular perspective, in *Coccolithophores: From molecular processes to global impact*, edited by H. R. Thierstein and J. R. Young, Springer-Verlag Berlin Heidelberg.

Cassar, N., Laws, E. A., and Popp, B. N. (2006), Carbon isotopic fractionation by the marine diatom *Phaeodactylum tricornutum* under nutrient- and light-limited growth conditions, *Geochimica et Cosmochimica Acta, 70,* 5323-5335.

Dong, L. F., N. A. Nimer, E. Okus, and M. J. Merrett (1993), Dissolved inorganic carbon utilization in relation to calcite production in *Emiliania huxleyi* (Lohmann) Kamptner, *New Phytology*, *123*, 679-684.

Dudley, W. C., and D. E. Goodney (1979), Oxygen isotope analyses of coccoliths grown in culture, *Deep Sea Research A*, *26*, 495-503.

Dudley, W. C., J. C. Duplessy, P. L. Blackwelder, L. E. Brand, and R. R. L. Guillard (1980), Coccoliths in Pleistocene-Holocene nannofossil assemblages, *Nature*, *285*, 222-223.

Dudley, W. C., P. Blackwelder, L. Brand, and J. C. Duplessy (1986), Stable isotopic composition of coccoliths, *Marine Micropaleontology*, *10*, 1-8.

Duplessy J. C., C. Lalou, and A. C. Vinot (1970), Differential isotopic fractionation in benthic foraminifera and paleotemperatures re-assessed, *Science*, *168***,** 250-251.

Erez, J. (1978), Vital effect on stable-isotope composition seen in Foraminifera and coral skeletons, *Nature*, *273*, 199-202.

Fairbanks, R. G., M. Sverdlove, R. Free, P. H. Wiebe, and A. W. H. Bé (1982), Vertical distribution and isotopic fractionation of living planktonic Foraminifera from the Panama Basin, *Nature*, *298*, 841-844.

Falkowski, P. G., M. E. Katz, A. H. Knoll, A. Quigg, J. A. Raven, O. Schofield, and F. J. R. Taylor (2004), The Evolution of Modern Eukaryotic Phytoplankton, *Science*, *305*(5682), 354-360.

Falkowski, P. G., and J. A. Raven (2007), *Aquatic Photosynthesis 2nd Edition*, Princeton University Press, Princeton, USA.

Flores, J.-A., M. A. Bárcena, and F. J. Sierro (2000), Ocean-surface and wind dynamics in the Atlantic Ocean off Northwest Africa during the last 140 000 years, *Paleogeography, Palaeoclimatology, Palaeoecology*, *161*, 459-478.

Foster, G. L. (2008), Seawater pH, pCO_2 and [CO_2^{3-}] variations in the Caribbean Sea over the last 130 kyr: a boron isotope and B/Ca study of planktic Foraminifera, *Earth and Planetary Science Letters*, *271*(1-4), 254–266.

Gervais, F., and U. Riebesell (2001), Effect of phosphorus limitation on elemental composition and stable carbon isotope fractionation in a marine diatom growing under different CO_2 concentrations, *Limnology and Oceanography, 46(3)*, 497-504.

Gibbs, S., N. Shackleton, and J. Young (2004), Identification of dissolution patterns in nannofossil assemblages: A high-resolution comparison of synchronous records from Ceara Rise, ODP Leg 154, *Paleoceanography, 19*, PA1029.

Gibbs, S. J., H. M. Stoll, P. Bown, and T. J. Bralower (2010), Ocean acidification and surface water carbonate production across the Paleocene-Eocene thermal maximum, *Earth and Planetary Science Letters*, *295*, 583-592.

Giordano, M., J. Beardall, and J. A. Raven (2005), CO_2 Concentrating Mechanisms in Algae: Mechanisms, Environmental Modulation, and Evolution, *Annual Reviews in Plant Biology*, *56*, 99-131.

Groeneveld, J. (2005), Effect of the Pliocene closure of the Panamanian Gateway on Caribbean and east Pacific sea surface temperatures and salinities by applying combined Mg/Ca and $\delta^{18}O$ measurements (5.6-2.2 Ma), *PhD Thesis*, IFM-Geomar, Kiel, Germany.

Grossman, E. L. (1987), Stable isotopes in modern benthic Foraminifera: a study of vital effect, *Journal of Foraminiferal Research*, *17*(1), 48-61.

Haug, G. H., and R. Tiedemann (1998), Effect of the formation of the Isthmus of Panama on Atlantic Ocean thermohaline circulation, *Nature*, *393*, 673-677.

Henderiks, J. (2008), Coccolithophore size rules - Reconstructing ancient cell geometry and cellular calcite quota from fossil coccoliths, *Marine Micropaleontology*, *67*, 143-154.

Henderiks, J., and M. Pagani (2008), Coccolithophore cell size and the Paleogene decline in atmospheric CO_2, *Earth and Planetary Science Letters*, *269*, 576-584.

Herrmann, S. and H.R. Thierstein (2012), Cenozoic coccolith size changes-Evolutionary and/or ecological controls? *Palaeogeography, Palaeoclimatology, Palaeoecology, 333-334*, 92-106.

Honjo, S., and H. Okada (1974), Community structure of coccolithophores in the photic layer of the med-Pacific, *Micropaleontology*, *20*(2), 209-230.

Janofske, D. (1992), Calcareous nannofossils of the Alpine Upper Triassic, in *Nannoplankton Research*, edited by B. Hamrsmid and J. R. Young, pp. 87-109, Knihovnicka ZPZ.

John, C. M., S. M. Bohaty, J. C. Zachos, A. Sluijs, S. J. Gibbs, H. Brinkhuis, and T. J. Bralower (2008), North American continental margin records of the Paleocene–Eocene thermal maximum: implications for global carbon and hydrological cycling, *Paleoceanography*, *23*, PA2217.

Kleiven, H. F., E. Jansen, T. Fronval, and T. M. Smith (2002), Intensification of Northern hemisphere glaciations in the circum Atlantic region (3.5-2.4 Ma) -

ice-rafted detritus evidence, *Palaeogeography, Palaeoclimatology, Palaeoecology*, *184*, 213-223.

Kopp, R. E., D. Schumann, T. D. Raub, D. S. Powars, L. V. Godfrey, N. L. Swanson-Hysell, A. C. Maloof, and H. Vali (2009), An Appalachian Amazon? Magnetofossil evidence for the development of a tropical river-like system in the mid-Atlantic United States during the Paleocene-Eocene thermal maximum, *Paleoceanography*, *24*, PA4211.

Langer, G., M. Geisen, K.-H. Baumann, J. Kläs, U. Riebesell, S. Thoms, and J. R. Young, (2006), Species-specific responses of calcifying algae to changing seawater carbonate chemistry, *Geochemistry, Geophysics, Geosystems*, *7*, Q09006.

Lawrence, K. T., T. D. Herbert, C. M. Brown, M. E. Raymo, and A. M. Haywood (2009), High-amplitude variations in North Atlantic sea surface temperature during the early Pliocene warm Period, *Paleoceanography*, *24*(doi:10.1029/2008PA001669).

Lisiecki, L. E., and M. E. Raymo (2005), A Pliocene-Pleistocene stack of 57 globally distributed benthic delta-18 O records, *Paleoceanography*, *20*, PA1003.

Margolis, S. V., P. Kroopnick, D. E. Goodney, W. C. Dudley, and M. E. Mahoney (1975), Oxygen and carbon isotopes from calcareous nannofossils as paleoceanographic indicators, *Science*, *189*(4202), 555-557.

McConnaughey, T. A. (1989a), ^{13}C and ^{18}O isotopic disequilibrium in biological carbonates; I. Patterns, *Geochimica y Cosmochimica Acta*, *53*, 151-162.

McConnaughey, T. A. (1989b), ^{13}C and ^{18}O isotopic disequilibrium in biological carbonates; II, In vitro simulation of kinetic isotope effects, *Geochimica y Cosmochimica Acta, 53*, 163-171.

Miller, K. G., et al. (1998), *Proceedings of the Ocean Drilling Program, Initial Reports, Leg 174AX*, Ocean Drilling Program, College Station, Texas.

Miller, K. G., P. J. Sugarman, J. V. Browning, M. A. Kominz, R. K. Olsson, M. D. Feigenson, and J. C. Hernandez (2004), Upper Cretaceous sequences and sea-level history, New Jersey coastal plain, *Geological Society of America Bulletin*, *116*, 368-393.

Moolna, A., and R. E. M. Rickaby (2012), Interaction of the coccolithophore *Gephyrocapsa oceanica* with its carbon environment: response to a recreated high-CO_2 geological past, *Geobiology*, *10*, 72–81.

Nimer, N. A., G. K. Dixon, and M. J. Merrett (1992), Utilization of inorganic carbon by the coccolithophorid *Emiliania huxleyi* (Lohmann) Kamptner, *New* Phytology, *120***,** 153-158.

Okada, H., and S. Honjo (1973), The distribution of oceanic coccolithophorids in the Pacific, *Deep Sea Research and Oceanographic Abstracts*, *20*(4), 355-364.

Pagani, M., M. A. Arthur, and K. H. Freeman (1999), The Miocene evolution of atmospheric carbon dioxide, *Paleoceanography*, *14*, 273-292.

Pagani, M., J. C. Zachos, K. H. Freeman, B. Tipple, and S. Bohaty (2005), Marked decline in atmospheric carbon dioxide concentrations during the Paleogene, *Science*, *309*, 600-603.

Pagani, M., Z. Liu, J. LaRiviere, and A. C. Ravelo (2009), High Earth-system climate sensitivity determined from Pliocene carbon dioxide concentrations, *Nature Geoscience*, *3*, 27 - 30.

Paillard, D., L. Labeyrie, and P. Yiou (1996), Macintosh program performs time-series analysis, *Eos Trans. AGU*, *77*, 379.

Paull, C. K., and H. R. Thierstein (1987), Stable isotopic fractionation among particles in Quaternary coccolith-sized deep sea sediments, *Paleoceanography*, *2*, 423– 429.

Perch-Nielsen, K. (1985), Cenozoic calcareous nannofossils, in *Plankton Stratigraphy*, edited by H. M. Bolli, et al., pp. 427-554, Cambridge Univ. Press, Cambridge.

Pienaar, R. N. (1994), Ultrastructure and calcification of coccolithophores, in *Coccolithophores*, edited by A. Winter and W. G. Siesser, Cambridge University Press, Cambridge.

Popp, B. N., E. A. Laws, R. R. Bidigare, J. E. Dore, K. L. Hanson, and S. G. Wakeham (1998), Effect of phytoplankton cell geometry on carbon isotopic fractionation, *Geochimica y Cosmochimica Acta*, *62*, 69-77.

Quinn, P., M. Y. Cortes, and J. Bollmann (2005), Morphological variation in the deep ocean-dwelling coccolithophore *Florisphaera profunda* (Haptophyta), *European Journal of Phycology*, *40*(1), 123-133.

Rau, G. H., U. Riebesell, and D. Wolf Gladrow (1996), A model of photosynthetic C-13 fractionation by marine phytoplankton based on diffusive molecular CO_2 uptake, *Marine Ecology-Progress Series*, *133* (1-3), 275-285.

Raven, J. A., and A. M. Johnston (1991), Mechanisms of inorganic-carbon acquisition in marine phytoplankton and their implications for the use of other resources, *Limnology and Oceanography*, *36*(8), 1701-1714.

Raven, J. A. (1998), The twelfth Tansley Lecture. Small is beautiful: the picophytoplankton, *Functional Ecology*, *12*, 503–513.

Raven, J. A., M. Giordano and J. Beardall (2008), Insights into the evolution of CCMs from comparisons with other resource acquisition and assimilation processes, *Physiologia Plantarum*, *133*, 4-14.

Raymo, M. E., B. Grant, M. Horowitz, and G. H. Rau (1996), Mid-Pliocene warmth: stronger greenhouse and stronger conveyor, *Marine Micropaleontology*, *27*, 313-326.

Reinfelder, J. R. (2011), Carbon Concentrating Mechanisms in Eukaryotic Marine Phytoplankton, *Annual Review of Marine Science*, *3*, 291-315.

Rickaby, R. E. M., and D. P. Schrag (2002), Growth rate dependence of Sr incorporation during calcification of *Emiliania huxleyi*, *Global Biogeochemical Cycles*, *16*(1), 1006.

Rickaby, R. E. M., J. Henderiks, and J. N. Young (2010), Perturbing phytoplankton: response and isotopic fractionation with changing carbonate chemistry in two coccolithophore species, *Climate of the Past*, *6*, 771–785.

Röhl, U., T. Westerhold, T. J. Bralower, and J. C. Zachos (2007), On the duration of the Paleocene-Eocene thermal maximum (PETM), *Geochemistry Geophysics Geosystems*, *8*, Q12002.

Rohling, E. J., M. Sprovieri, T. Cane, J. S. L. Casford, S. Cooke, I. Bouloubassi, K. C. Emeis, R. Schiebel, M. Rogerson, A. Hayes, F. J. Jorissen, and D. Kroon

(2004), Reconstructing past planktic Foraminiferal habitiats using stable isotope data: a case history for Mediterranean sapropel S5, *Marine Micropaleontology, 50*, 89-123.

Rost, B., U. Riebesell, S. Burkhardt, and D. Sultemeyer (2003), Carbon acquisition of bloom-forming marine phytoplankton, *Limnology and Oceanography*, *48*, 55-67.

Royer, D. L. (2006), CO_2-forced climate thresholds during the Phanerozoic, *Geochimica y Cosmochimica Acta, 70*, 5665–5675.

Schmidt, M. W., H. J. Spero, and D. W. Lea (2004), Links between salinity variation in the Caribbean and North Atlantic thermohaline circulation, *Nature*, *428*, 160-164.

Schulz, K.G., B. Rost, S. Burkhardt, U. Riebesell , S. Thoms, and D.A. Wolf-Gladrow (2007), The effect of iron availability on the regulation of inorganic carbon acquisition in the coccolithophore *Emiliania huxleyi* and the significance of cellular compartmentation for stable carbon isotope fractionation, *Geochimica et Cosmochimica Acta, 71*, 5301-5312.

Sciandra, A., J. Harlay, D. Lefevre, R. Lemee, P. Rimmelin, M. Denis and J-P. Gattuso (2003), Response of coccolithophorid *Emiliania huxleyi* to elevated partial pressure of CO_2 under nitrogen limitation. *Marine Ecology Progress Series*, 261, 111-22.

Seki, O., G. L. Foster, D. N. Schmidt, A. Mackensen, K. Kawamura, and R. D. Pancost (2010), Alkenone and boron-based Pliocene pCO_2 records, *Earth and Planetary Science Letters*, *292*, 201–211.

Shackleton, N. J., J. D. H. Wiseman, and H. A. Buckley (1973), Non-equilibrium **i**sotopic **f**ractionation between **s**eawater and **p**lanktonic **f**oraminiferal **t**ests**,** *Nature***,** *242*, 177-179**.**

Shackleton, N. J., J. Backman, H. Zimmerman, D. V. Kent, M. A. Hall, D. G. Roberts, D. Schnitker, and J. Baldauf (1984), Oxygen isotope calibration of the onset of ice-rafting and history of glaciation in the North Atlantic region, *Nature*, *307*, 620-623.

Shipboard Scientific Party (1997), Site 999, in *Proceedings of the Ocean Drilling Program, Initial Reports, Vol. 165*, edited by H. Sigurdsson, et al.

Sluijs, A. (2006), Global change during the Paleocene-Eocene thermal maximum, *PhD Thesis*, Utrecht University, The Netherlands.

Sluijs, A., H. Brinkhuis, S. Schouten, S. M. Bohaty, C. M. John, J. C. Zachos, G.-J. Reichart, J. S. S. Damsté, E. M. Crouch, and G. R. Dickens (2007), Environmental precursors to rapid light carbon injection at the Palaeocene/Eocene boundary, *Nature, 450*, 1218-1222.

Spero H. J., J. Bijma, D.W. Le, and B. E. Bemis (1997), Effect of seawater carbonate concentration on foraminiferal carbon and oxygen isotopes, *Nature, 390***,** 497-500.

Spero, H. J. 1998. Life history and stable isotope geochemistry of planktonic foraminifera, In: Norris, R. D. & Corfield, R. M. (eds) *Isotope Paleobiology and Paleoecology*; *Paleontological Society Papers*, *4*, 7-36.

Steinmetz, J. (1994), Stable isotopes in modern coccolithophores, in *Coccolithophores*, edited by A. Winter and W. G. Siesser, Cambridge University Press, Cambridge.

Steph, S. (2005), Pliocene stratigraphy and the impact of Panama uplift on changes in Caribbean and tropical east Pacific upper ocean stratification (6-2.5 Ma), *PhD Thesis*, IFM-Geomar, Kiel, Germany.

Steph, S., R. Tiedemann, M. Prange, J. Groeneveld, D. Nürnberg, L. Reuning, M. Schulz, and G. H. Haug (2006), Changes in Caribbean surface hydrography during the Pliocene shoaling of the Central American Seaway, *Paleoceanography*, *21*, PA4221.

Steph, S., M. Regenberg, R. Tiedemann, S. Mulitza, and D. Nürnberg (2009), Stable isotopes of planktonic Foraminifera from tropical Atlantic/Caribbean core-tops: Implications for reconstructing upper water column stratification, *Marine Micropaleontology*, *71*, 1-19.

Stoll, H. M., and D. P. Schrag (2000), Coccolith Sr/Ca ratios as a new indicator of coccolithophorid calcification and growth rate, *Geochemistry Geophysics Geosystems*, *1*, 1999GC000015.

Stoll, H. M., C. Klaas, I. Probert, J. Ruiz Encinar, and J. I. Garcia Alonso (2002), Calcification rate and temperature effects on Sr partitioning in coccoliths of multiple species of coccolithophorids in culture, *Global and Planetary Change*, *34*, 153-171.

Stoll, H. M., and P. Ziveri (2002), Methods for separation of monospecic coccolith samples from sediments, *Marine Micropaleontology*, *46*, 209-221.

Stoll, H. M. (2005), Limited range of interspecific vital effects in coccolith stable isotopic records during the Paleocene-Eocene thermal maximum, *Paleoceanography*, *20*, PA1007.

Stoll, H. M., A. Arevalos, A. Burke, P. Ziveri, G. Mortyn, N. Shimizu, and D. Unger (2007a), Seasonal cycles in biogenic production and export in Northern Bay of Bengal sediment traps, *Deep Sea Research Part II*, *54*, 558-580.

Stoll, H. M., N. Shimizu, A. Arevalos, N. Matell, A. Banasiak, and S. Zeren (2007b), Insights on coccolith chemistry from a new ion probe method for analysis of individually picked coccoliths, *Geochemistry Geophysics Geosystems*, *8*(6).

Stoll, H. M., P. Ziveri, N. Shimizu, M. Conte, and S. Theroux (2007c), Relationship between coccolith Sr/Ca ratios and coccolithophore production and export in the Arabian Sea and Sargasso Sea, *Deep Sea Research Part II*, *54*, 581-600.

Stoll, H. M., and N. Shimizu (2009), Micropicking of nannofossils in preparation for analysis by secondary ion mass spectrometry, *Nature Protocols*, *4*, 1038-1043.

Takahashi, T., S. C. Sutherland, R. Wanninkhof, C. Sweeney, R. A. Feely, D. W. Chipman, B. Hales, G. Friederich, F. P. Chavez, C. Sabine, A. J. Watson, D. C. E. Bakker, U. Schuster, N. Metzl, H. Yoshikawa-Inoue, M. Ishii, T. Midorikawa, Y. Nojiro, A. Kortzinger, T. Steinhoff, M. Hoppema, J. Olafsson, T. S. Arnarson, B. Tilbrook, T. Johannessen, A. Olsen, R. Bellerby, C. S. Wong, B. Delille, N. Bates, and H. J. W. de Baar (2009), Climatological mean and decadal change in surface ocean pCO_2, and net sea–air CO_2 flux over the global oceans, *Deep Sea Research Part II*, *56*, 554-577.

Tortell, P. D. (2000), Evolutionary and ecological perspectives on carbon acquisition in phytoplankton, *Limnology and Oceanography*, *45*, 744-750.

Trimborn, S., G. Langer, and B. Rost (2007), Effect of varying calcium concentrations and light intensities on calcification and photosynthesis in *Emiliania huxleyi*, *Limnology and Oceanography*, *52(5)*, 2285-2293.

Weber, J. N., and P.M.J. Woodhead (1972), Temperature Dependence of Oxygen-18 Concentration in Reef Coral Carbonates, *Journal of Geophysical Research, 77*(3), 463-473.

Weiner, S., and P. M. Dove (2003), An overview of biomineralization processes and the problem of the vital effect, in *Biomineralization*, edited by P. M. Dove, et al., Mineralogical Society of America and The Geochemical Society, Washington DC.

Young, J., and P. Ziveri (2000), Calculation of coccolith volume and its use in calibration of carbonate flux estimates, *Deep Sea Research Part II, 47*, 1679–1700.

Young, J., K. Henriksen, and I. Probert (2004), Structure and morphogenesis of the coccoliths of the CODENET species, in *Coccolithophores: From molecular processes to global impact*, edited by H. R. Thierstein and J. Young, Springer-Verlag Berlin Heidelberg.

Young, J. R. (1998), Neogene, in *Calcareous Nannofossil Biostratigraphy*, edited by P. Bown, pp. 225-265, Chapman & Hall, Cambridge.

Young, J. N., R. E. M. Rickaby, M. V. Kapralov and D. A. Filatov (2012), Adaptive signals in algal Rubisco reveal a history of ancient atmospheric carbon dioxide, *Philosophical Transactions of the Royal Society B, 367*, 483-492.

Zachos, J. C., Röhl, U., Schellenberg, S. A. et al. (2005), Rapid Acidification of the Ocean during the Paleocene–Eocene Thermal Maximum, *Science*, *308*, 1611-1615.

Zachos, J. C., G. R. Dickens, and R. E. Zeebe (2008), An early Cenozoic perspective on greenhouse warming and carbon-cycle dynamics, *Nature*, *451*, 279-283.

Zeebe, R. E. (1999), An explanation of the effect of seawater carbonate concentration on foraminiferal oxygen isotopes, *Geochimica et Cosmochimica Acta*, 63 (13/14), 2001-2007.

Zeebe, R. E., D.A. Wolf-Gladrow, and H. Jansen (1999), On the time required to establish chemical and isotopic equilibrium in the carbon dioxide system in seawater, *Marine Chemistry*, *65*, 135-153.

Zeebe, R. E., and D. A. Wolf-Gladrow (2001), *CO_2 in Seawater: Equilibrium, Kinetics, Isotopes*, Elsevier, Amsterdam.

Zeebe, R.E., J. Bijma, B. Hönisch, A. Sanyal, H.J. Spero, and D.A. Wolf-Gladrow (2008), Vital effects and beyond: a modelling perspective on developing palaeoceanographical proxy relationships in foraminifera, In Austin, W. E. N. & James, R. H. (eds) *Biogeochemical Controls on Palaeoceanographic Environmental Proxies. Geological Society, London, Special Publications, 303*, 45-58.

Ziveri, P., H. M. Stoll, I. Probert, C. Klaas, M. Geisen, G. Ganssen, and J. Young (2003), Stable isotope 'vital effects' in coccolith calcite, *Earth and Planetary Science Letters*, *210*, 137-149.

Ziveri, P., S. Thoms, I. Probert, M. Geisen, and G. Langer (2012), A universal carbonate ion effect on stable oxygen isotope ratios in unicellular planktonic calcifying organisms, *Biogeosciences, 9,* 1025-1032.

Figure Captions

Table 1: Main constituents of coccolith size fractions expressed as carbonate contribution at Bass River during the PETM in six samples covering the interval of

maximum change in bulk $\delta^{13}C$. Placoliths are grouped into three size categories (see section 3.1 for species' details). Where one group/genus heavily dominates carbonate, values are in bold.

Table 2: Main constituents of coccolith size fractions expressed as carbonate contribution at Site 999 for PPT samples 2 (2180 ka), 9 (2660 ka) and 21 (3392 ka) and LGM sample. Values are only shown where contribution exceeds 10%. Where one species or genus heavily dominates carbonate, values are in bold.

Figure 1: A: relationship between oxygen isotopic fractionation and cell size in cultured coccolithophores of multiple species (cultures at pH 7.6 ± 0.15 in natural seawater, DIC not determined). Data from *Ziveri et al*. [2003]. B: Contraction of range of vital effects between small (*Gephyrocapsa oceanica*) and large (*Coccolithus pelagicus ssp. braarudii*) coccoliths at higher culture $CO_{2(aq)}$. Data from *Rickaby et al.* [2010], where low CO_2 is 10-15 µmol/kg and high CO_2 is 60 µmol/kg. We note that in DIC experiments, consequences on coccolith $\delta^{18}O$ may not be identical to those expected in the paleo-ocean because no parallel pH change occurs, whereas during past Cenozoic pCO_2 changes variations in pH are predicted to have accompanied DIC changes. C: Expansion of the range of vital effects at higher growth rates. Data from *Ziveri et al*. [2003].

Figure 2: Plio-Pleistocene climate over the past 5 m.y. A: LR04 benthic $\delta^{18}O$ stack [*Lisiecki and Raymo*, 2005] (note inverted axis). B: Plio-Pleistocene pCO_2 estimates from ODP Site 999. Maximum and minimum pCO_2 based on alkenone $\delta^{13}C$ [*Seki et al*., 2010, green shading]; and $\delta^{11}B$ of the Foraminifera *G. sacculifer* [*Bartoli et al*.,

2011; glacial and interglacial data shown; light blue shading) and *G. ruber* [*Seki et al.*, 2010; dark blue lines]. Dashed dark blue line is pCO_2 determined from pH and assuming a modern value for total alkalinity (5% uncertainty on TA value); solid dark blue line is pCO_2 determined from pH and modern [CO_3^{2-}] (±25 ppm error) [*Seki et al.*, 2010]. Grey box denotes our PPT study interval.

Figure 3: Description of size separation protocol for Site 999 coccoliths. For each step, 'a' (squares) represents the sediment at the bottom of the settling column and 'b' (circles) represents the particles still in suspension. During step 4, the resultant supernatant was additionally filtered at 10μm to reduce contamination of large *Helicosphaera* coccoliths by foram fragments and *Discoaster*. Mean PPT percentage carbonate contribution values are quoted in brackets for each fraction (See Table 2).

Figure 4: Coccolith isotopes and Sr/Ca ratios over the PETM at Bass River. A: $\delta^{18}O$ and B: $\delta^{13}C$ for small and medium-sized coccoliths. Also shown in A and B are stable isotope records for bulk carbonate, benthic Foraminifera *Cibicidoides* sp., and planktic Foraminifera *Acarinina* sp (bulk and foram data from *John et al.*, [2008]). C: Coccolith Sr/Ca ratios for small and medium sized *Toweius* and large *Coccolithus* coccoliths, D: The ratio between Spiniferite and *Areoligera* dinoflagellate cysts (=S/(S+A)), related to salinity and sea level [*Sluijs et al.*, 2006]. Note inverted axis.

Figure 5: Coccolith stable isotopes at Site 999 during the PPT (3.5-2 Ma) in the context of climate; A: Site 999 benthic foraminiferal $\delta^{18}O$ (corrected to equilibrium by adding 0.64‰) [*Haug & Tiederman*, 1998] (inverted axis). B: pCO_2 estimates from Site 999 (same colour coding and data sources as Fig. 1. NB: only interglacial

data from *Bartoli et al*., [2011] are shown here). C & D: Coccolith size-fraction $\delta^{18}O$ (C) and $\delta^{13}C$ (D) normalised to isotope values of the Foraminifer *Globigerinoides sacculifer* from the same samples (PPT $\delta^{18}O$ from *Haug et al.* [2001] and $\delta^{13}C$ from *J. Groeneveld* [unpublished data]; LGM data from S*chmidt et al*. [2004]). *G. sacculifer* is assumed to be recording mixed layer conditions in equilibrium in the Caribbean at ~100m mean depth [*Steph et al.,* 2006; *Steph et al.,* 2009 their Fig. 4a and references in figure caption therein]. LGM coccolith isotope data are also shown on the left of panels C and D.

Figure 6: Crossplots of $\delta^{18}O$ versus $\delta^{13}C$ for coccolith size fractions at Site 999. A: mean values for the PPT, B, C and D: 3-sample mean values from young, middle and older portions of the PPT record (all normalised to *G. sacculifer* as in Fig. 4). E: LGM sample (duplicate sample splits analysed, also normalised to *G. sacculifer*). NB: axis scales and breaks are different in panel E (LGM) compared to A-D because of the very negative isotopic composition of *Thoracosphaeraceae* (red circle), which is not included in calculations of the range of coccolith isotopic values because it is a dinocyst and not a coccolith signature.

Figure 7: PPT coccolith productivity and inter-fraction isotopic differences. A: Sr/Ca ratios (dashed lines) and productivity residuals (solid lines) for two coccolith fractions (2b: small reticulofenestrids and 4b: *Helicosphaera*). B: *N ratio* floral record. For both proxies, higher values indicate higher coccolithophore productivity. C: the difference in isotopic composition between small reticulofenestrids and *Helicosphaera* coccolith size-fractions. LGM differences are shown on the left.

Figure 8: Site 999 PPT mean coccolith isotope values (black symbols, pink shading) plotted with Foraminifera isotopes (blue symbols, blue shading) in 'Foraminifera depth habitat space'. Foraminifera data are also from peak interglacials and averaged over the same time interval. *N. dutertrei* and *G. limbata* data from *Steph* [2005], *Cibicidoides* sp. data from *Haug and Tiedemann* [1998], and *G. sacculifer* data from *Groeneveld* [2005].

Figure 9: Mean Bass River PETM coccolith isotope values (black symbols, pink shading) plotted with Foraminifera (blue symbols, blue shading) and bulk sediment (green symbol) isotope data. Foraminifera and bulk data from *John et al*. [2008]. Interval for averaging (356.02 to 359.4 metres) was chosen based on where both coccolith and Foraminifera data were available so as not to bias mean values.

Table 1

PETM Bass River — Percent carbonate contribution (%)

Size fraction	Genera/Group	356.95m	357.1m	357.38m	357.56m	357.74m	357.9m	Mean PETM
1b	v. small coccolith fragments	7.2	10.9	4.4	6.1	13.9	10.6	8.8
1.5-5µm	V. Small placoliths (mean diameter 1.5µm)	**26.1**	**59.4**	13.0	**53.6**	**50.6**	**33.8**	**39.4**
	Small placoliths (mean diameter 2.7µm)	**64.3**	**27.1**	**79.8**	**36.8**	**32.4**	**50.7**	**48.5**
	Medium placoliths (mean diameter 5µm)	2.4	2.6	2.8	3.5	3.1	5.0	3.2
1ax	V. Small placoliths (mean diameter 1.5µm)	1.2	0.5	1.1	1.4	3.5	1.3	1.5
5-8µm	Small placoliths (mean diameter 2.7µm)	7.2	4.8	6.9	14.2	**28.4**	7.1	11.4
	Medium placoliths (mean diameter 5µm)	**91.6**	**78.8**	**74.9**	**71.5**	**39.5**	**91.6**	**74.6**
	Discoaster	0.0	15.9	17.1	12.9	0.0	0.0	7.7
	Chiasmolithus	0.0	0.0	0.0	0.0	**28.6**	0.0	4.8
1a	V. Small placoliths (mean diameter 1.5µm)	0.1	0.1	0.1	0.3	0.1	0.1	0.1
8-20µm	Small placoliths (mean diameter 2.7µm)	0.5	1.3	0.4	0.7	0.6	0.9	0.7
	Medium placoliths (mean diameter 5µm)	4.8	5.9	3.4	5.9	4.1	5.4	4.9
	Large *Chiasmolithus*	11.3	17.1	8.9	25.6	14.4	12.9	15.0
	Large *Coccolithus*	9.1	7.1	8.1	6.2	11.5	9.4	8.6
	Discoaster	**43.3**	18.3	19.9	5.1	9.8	23.3	20.0
	Large Foraminifer Fragments	**31.0**	**50.2**	**59.2**	**56.2**	**59.4**	**48.0**	**50.7**

Table 2

PPT ODP Site 999 — Percent carbonate contribution (%)

Size fraction	Species/Genera	LGM	Pliocene 2	Pliocene 9	Pliocene 21	Mean Pliocene
1b	*Florisphaera profunda*	**65.4**	**74.4**	**83.9**	**73.7**	**77.3**
<2.5µm	*Reticulofenestra* (<3um)	-	25.6	16.1	26.3	22.7
	Gephyrocapsa + Emiliania (<3um)	34.6	-	-	-	-
2b	*Florisphaera profunda*	19.4	14.8	25.5	12.1	17.5
2.5-4µm	*Reticulofenestra + Pseudoemiliania* (<4um)		**85.2**	**74.5**	**87.9**	**82.5**
	Gephyrocapsa + Emiliania (<4um)	**80.6**				
3b	*Reticulofenestra + Pseudoemiliania* (<5um)	-	19.1	15.2	46.1	26.8
4-6µm	*Gephyrocapsa + Emiliania* (<5um)	43.2	-	-	-	-
(Mixed med.	*Umbilicosphaera*		19.4			
size coccoliths)	*Oolithotus fragilis* / Calcidiscus*	17.5		18.9		
	Helicosphaera small-med	12.0	42.5	26.6	11.1	26.7
	Discoaster				18.0	
4b	*Helicosphaera* med-large	30.2	**68.5**	**78.2**	**72.0**	**72.9**
6-9µm	Large *Gephyrocapsa* (>5um)	17.1				
	Rhabdosphaera	19.0				
	Oolithotus fragilis + Calcidiscus	17.8				
4bx	*Helicosphaera*		27.1	49.9	41.0	39.4
9-12µm	*Discoaster*			22.0	42.0	
	Thoracosphaera	**90.7**				
	Coccolithus pelagicus		57.4	13.6		

* LGM only

Figure 1

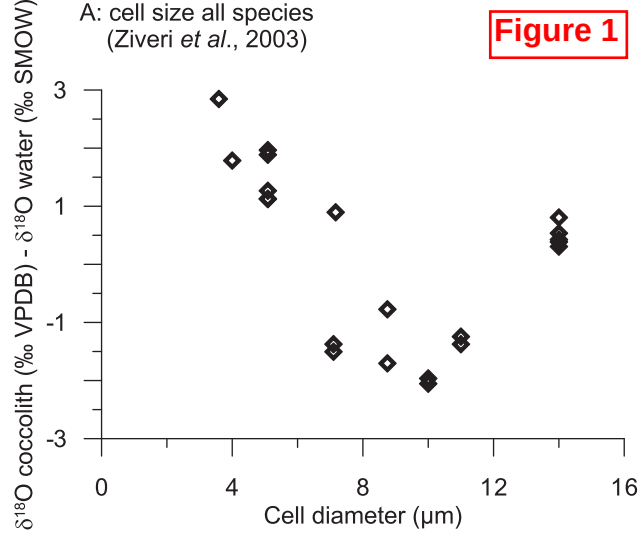
A: cell size all species
(Ziveri et al., 2003)
δ18O coccolith (‰ VPDB) - δ18O water (‰ SMOW)
3
1
-1
-3
0
4
8
12
16
Cell diameter (µm)

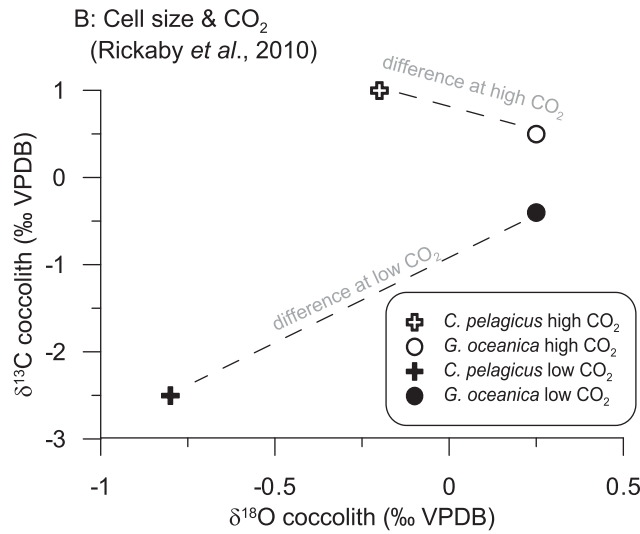
B: Cell size & CO2
(Rickaby et al., 2010)
difference at high CO2
difference at low CO2
C. pelagicus high CO2
G. oceanica high CO2
C. pelagicus low CO2
G. oceanica low CO2
δ13C coccolith (‰ VPDB)
1
0
-1
-2
-3
-1
-0.5
0
0.5
δ18O coccolith (‰ VPDB)

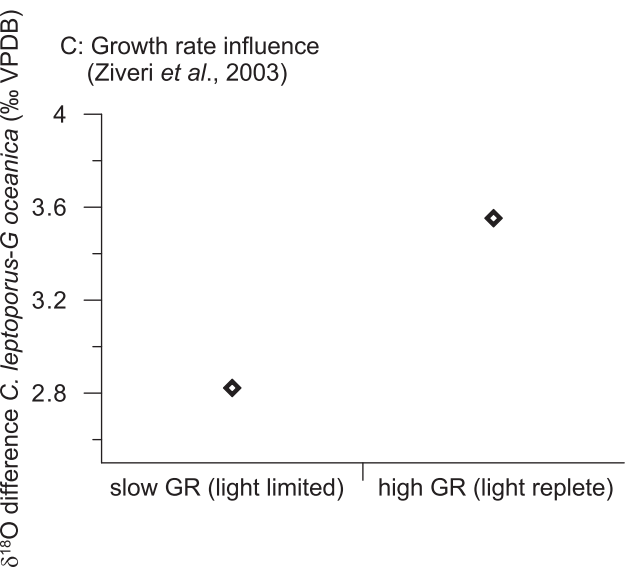
C: Growth rate influence
(Ziveri et al., 2003)
δ18O difference C. leptoporus-G oceanica (‰ VPDB)
4
3.6
3.2
2.8
slow GR (light limited)
high GR (light replete)

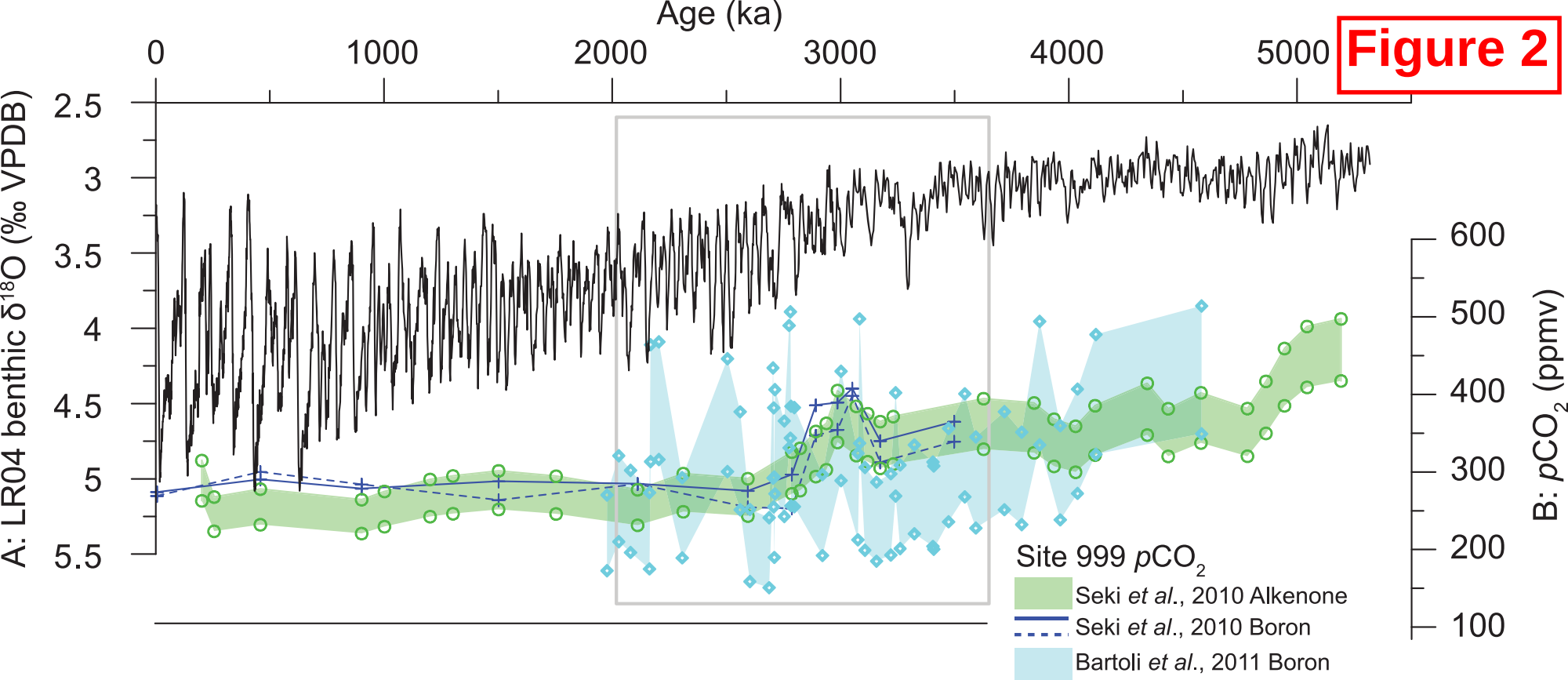
Figure 2
Age (ka)
0
1000
2000
3000
4000
5000
A: LR04 benthic δ18O (‰ VPDB)
2.5
3
3.5
4
4.5
5
5.5
B: pCO2 (ppmv)
600
500
400
300
200
100
Site 999 pCO2
Seki et al., 2010 Alkenone
Seki et al., 2010 Boron
Bartoli et al., 2011 Boron

Figure 3

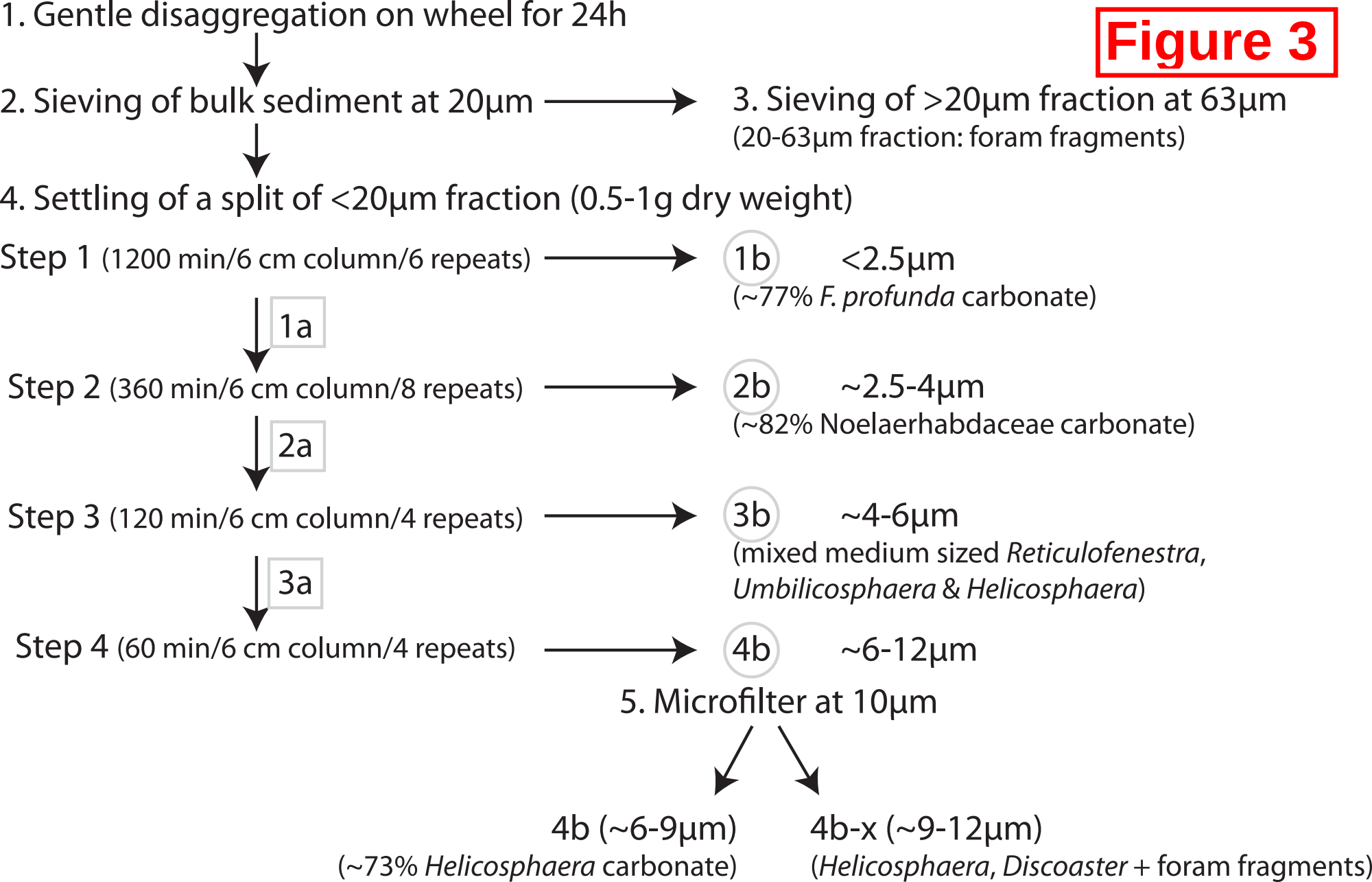
1. Gentle disaggregation on wheel for 24h
2. Sieving of bulk sediment at 20µm
3. Sieving of >20µm fraction at 63µm
(20-63µm fraction: foram fragments)
4. Settling of a split of <20µm fraction (0.5-1g dry weight)
Step 1 (1200 min/6 cm column/6 repeats)
1b <2.5µm
(~77% F. profunda carbonate)
1a
Step 2 (360 min/6 cm column/8 repeats)
2b ~2.5-4µm
(~82% Noelaerhabdaceae carbonate)
2a
Step 3 (120 min/6 cm column/4 repeats)
3b ~4-6µm
(mixed medium sized Reticulofenestra, Umbilicosphaera & Helicosphaera)
3a
Step 4 (60 min/6 cm column/4 repeats)
4b ~6-12µm
5. Microfilter at 10µm
4b (~6-9µm)
(~73% Helicosphaera carbonate)
4b-x (~9-12µm)
(Helicosphaera, Discoaster + foram fragments)

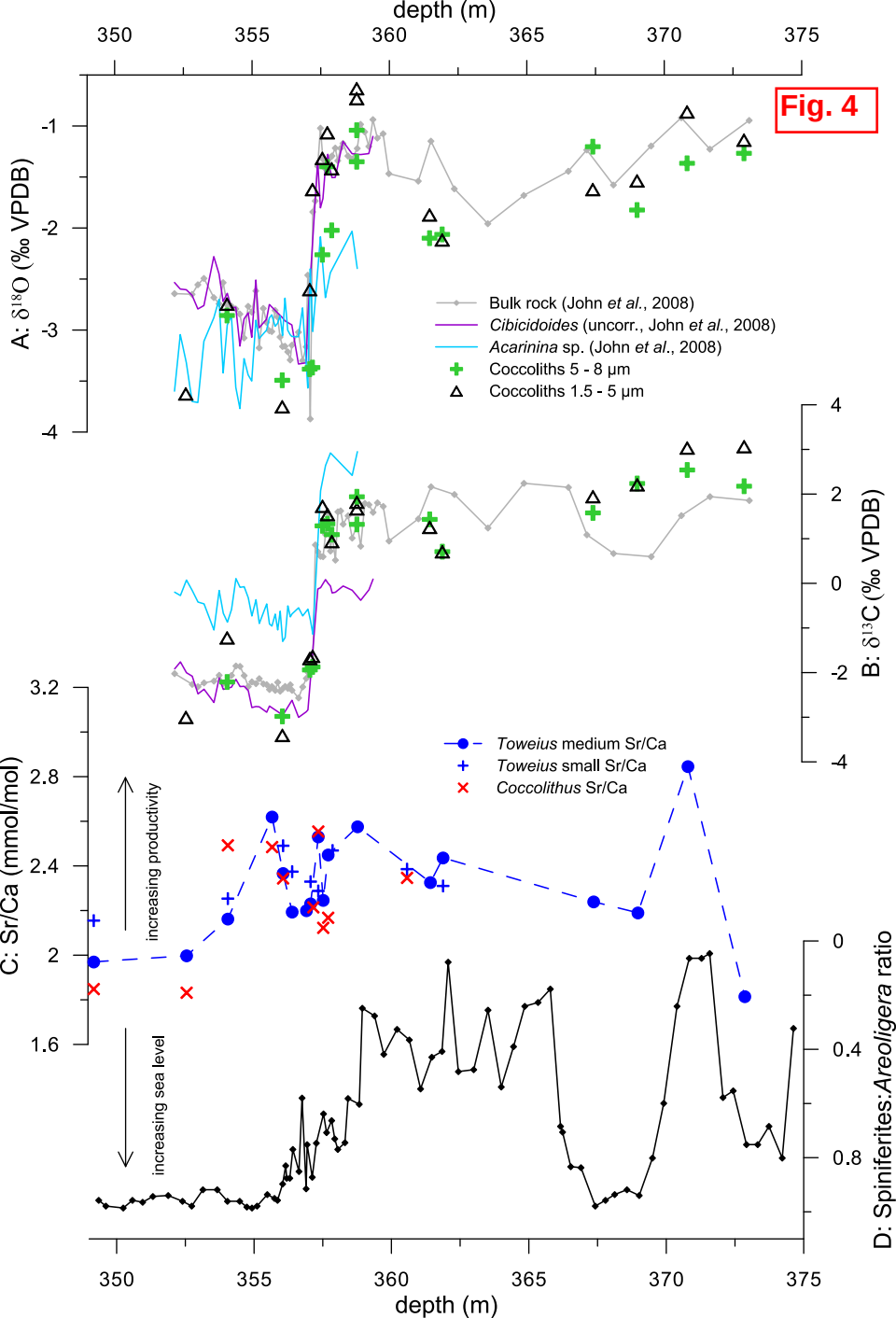
Fig. 4
depth (m)
350
355
360
365
370
375
A: δ18O (‰ VPDB)
-1
-2
-3
-4
Bulk rock (John et al., 2008)
Cibicidoides (uncorr., John et al., 2008)
Acarinina sp. (John et al., 2008)
Coccoliths 5 - 8 µm
Coccoliths 1.5 - 5 µm
B: δ13C (‰ VPDB)
4
2
0
-2
-4
C: Sr/Ca (mmol/mol)
3.2
2.8
2.4
2
1.6
Toweius medium Sr/Ca
Toweius small Sr/Ca
Coccolithus Sr/Ca
increasing productivity
increasing sea level
D: Spiniferites:Areoligera ratio
0
0.4
0.8
depth (m)

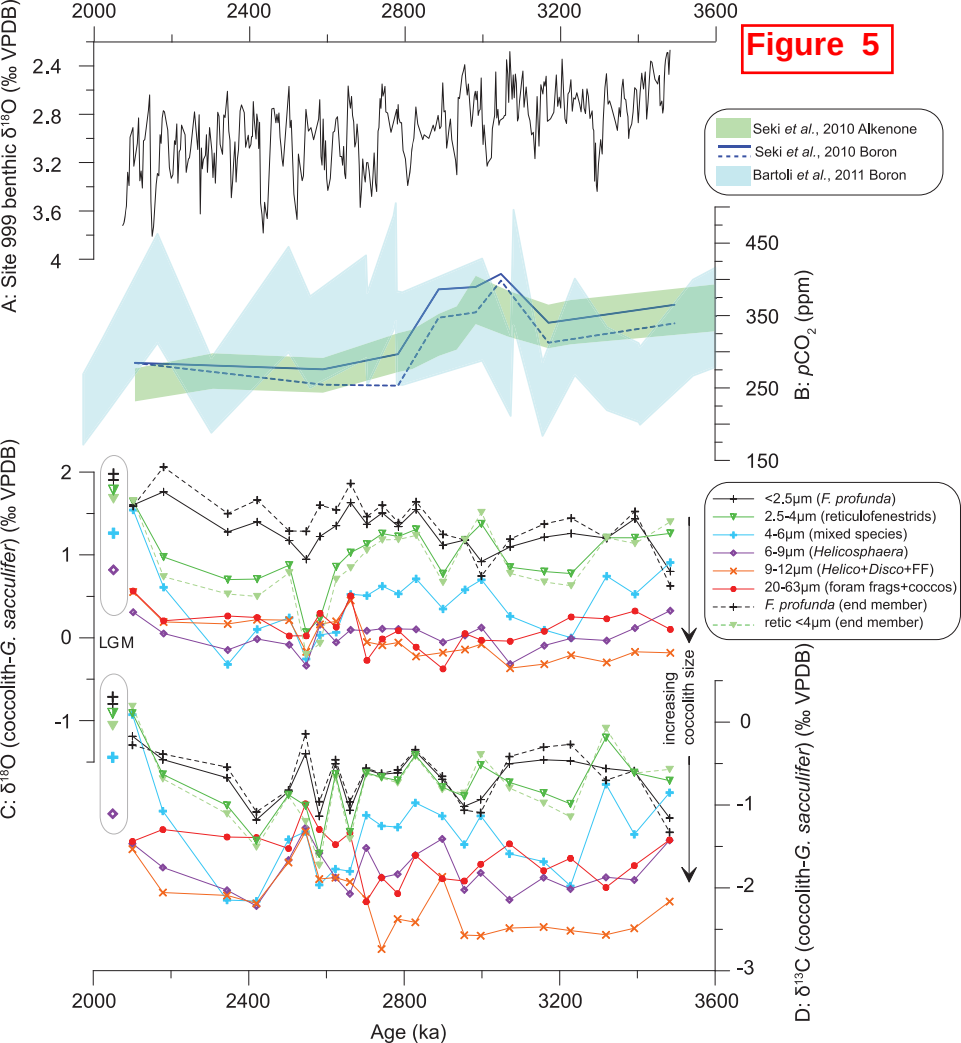
Figure 5
Seki et al., 2010 Alkenone
Seki et al., 2010 Boron
Bartoli et al., 2011 Boron
A: Site 999 benthic δ18O (‰ VPDB)
B: pCO2 (ppm)
C: δ18O (coccolith-G. sacculifer) (‰ VPDB)
D: δ13C (coccolith-G. sacculifer) (‰ VPDB)
<2.5µm (F. profunda)
2.5-4µm (reticulofenestrids)
4-6µm (mixed species)
6-9µm (Helicosphaera)
9-12µm (Helico+Disco+FF)
20-63µm (foram frags+coccos)
F. profunda (end member)
retic <4µm (end member)
LGM
increasing coccolith size
Age (ka)

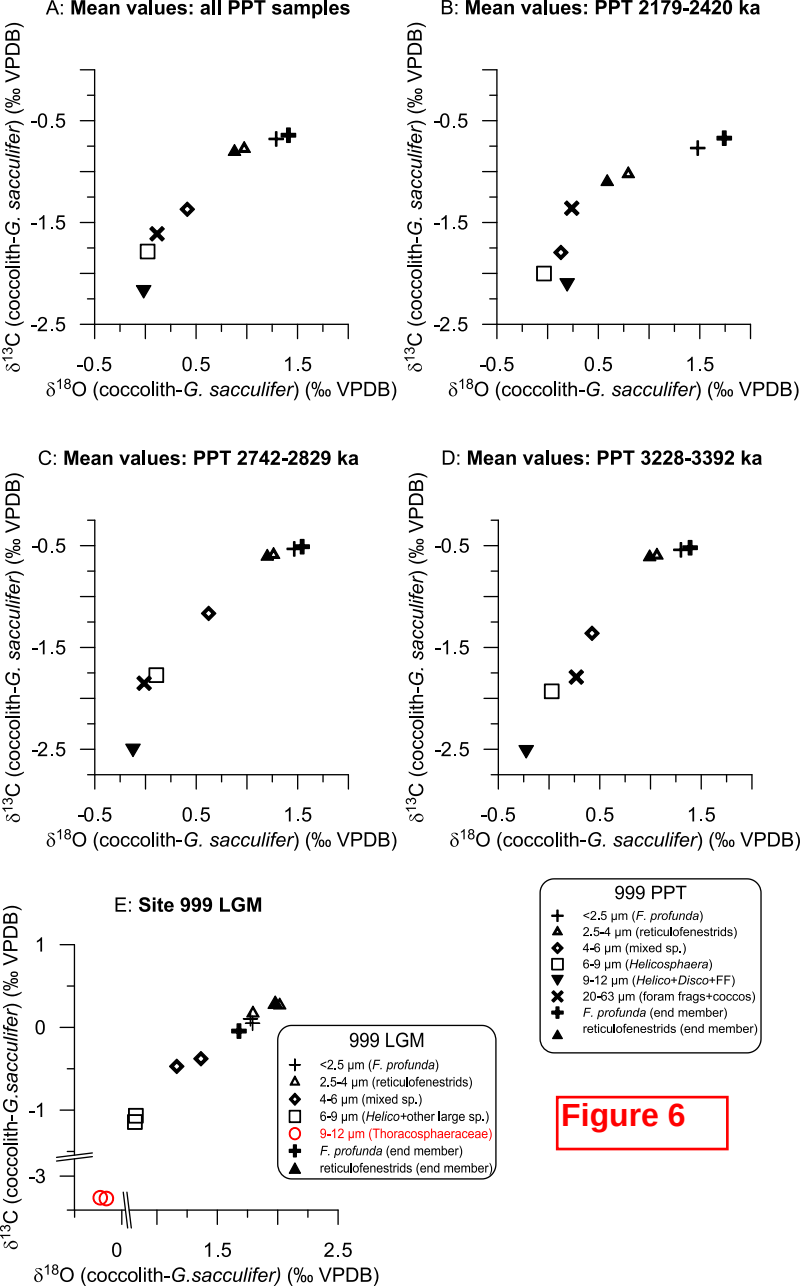
A: Mean values: all PPT samples
B: Mean values: PPT 2179-2420 ka
C: Mean values: PPT 2742-2829 ka
D: Mean values: PPT 3228-3392 ka
E: Site 999 LGM
δ13C (coccolith-G. sacculifer) (‰ VPDB)
δ18O (coccolith-G. sacculifer) (‰ VPDB)
-0.5
-1.5
-2.5
0.5
1.5
0
1
-1
-3
2.5
999 PPT
<2.5 µm (F. profunda)
2.5-4 µm (reticulofenestrids)
4-6 µm (mixed sp.)
6-9 µm (Helicosphaera)
9-12 µm (Helico+Disco+FF)
20-63 µm (foram frags+coccos)
F. profunda (end member)
reticulofenestrids (end member)
999 LGM
<2.5 µm (F. profunda)
2.5-4 µm (reticulofenestrids)
4-6 µm (mixed sp.)
6-9 µm (Helicosphaera+other large sp.)
9-12 µm (Thoracosphaeraceae)
F. profunda (end member)
reticulofenestrids (end member)

Figure 6

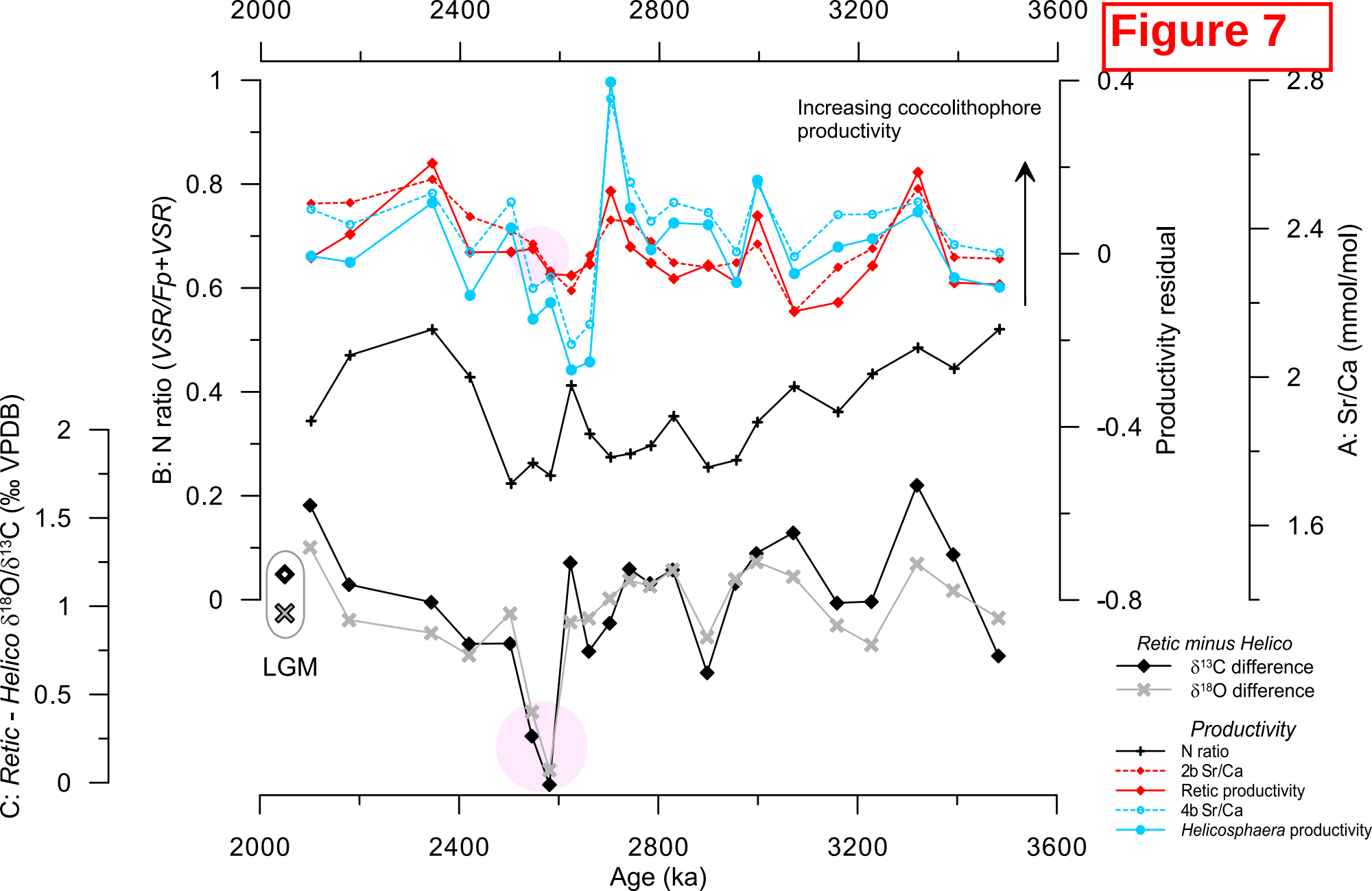
Figure 7
Increasing coccolithophore productivity
B: N ratio (VSR/Fp+VSR)
Productivity residual
A: Sr/Ca (mmol/mol)
C: Retic - Helico δ18O/δ13C (‰ VPDB)
Age (ka)
LGM
Retic minus Helico
δ13C difference
δ18O difference
Productivity
N ratio
2b Sr/Ca
Retic productivity
4b Sr/Ca
Helicosphaera productivity

PPT ODP Site 999
mean isotope values (interglacials 3.5-2 Ma)

Figure 8

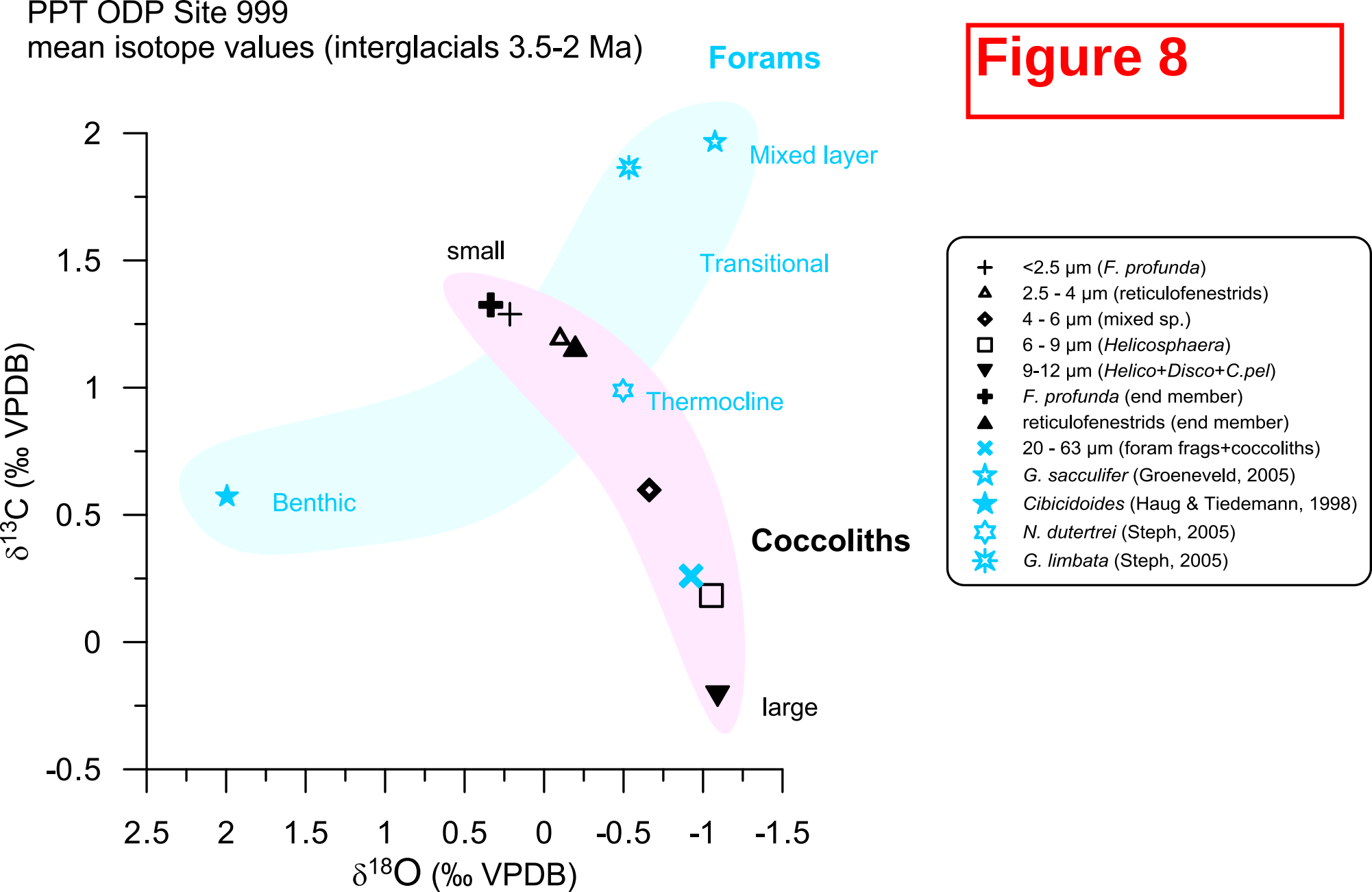

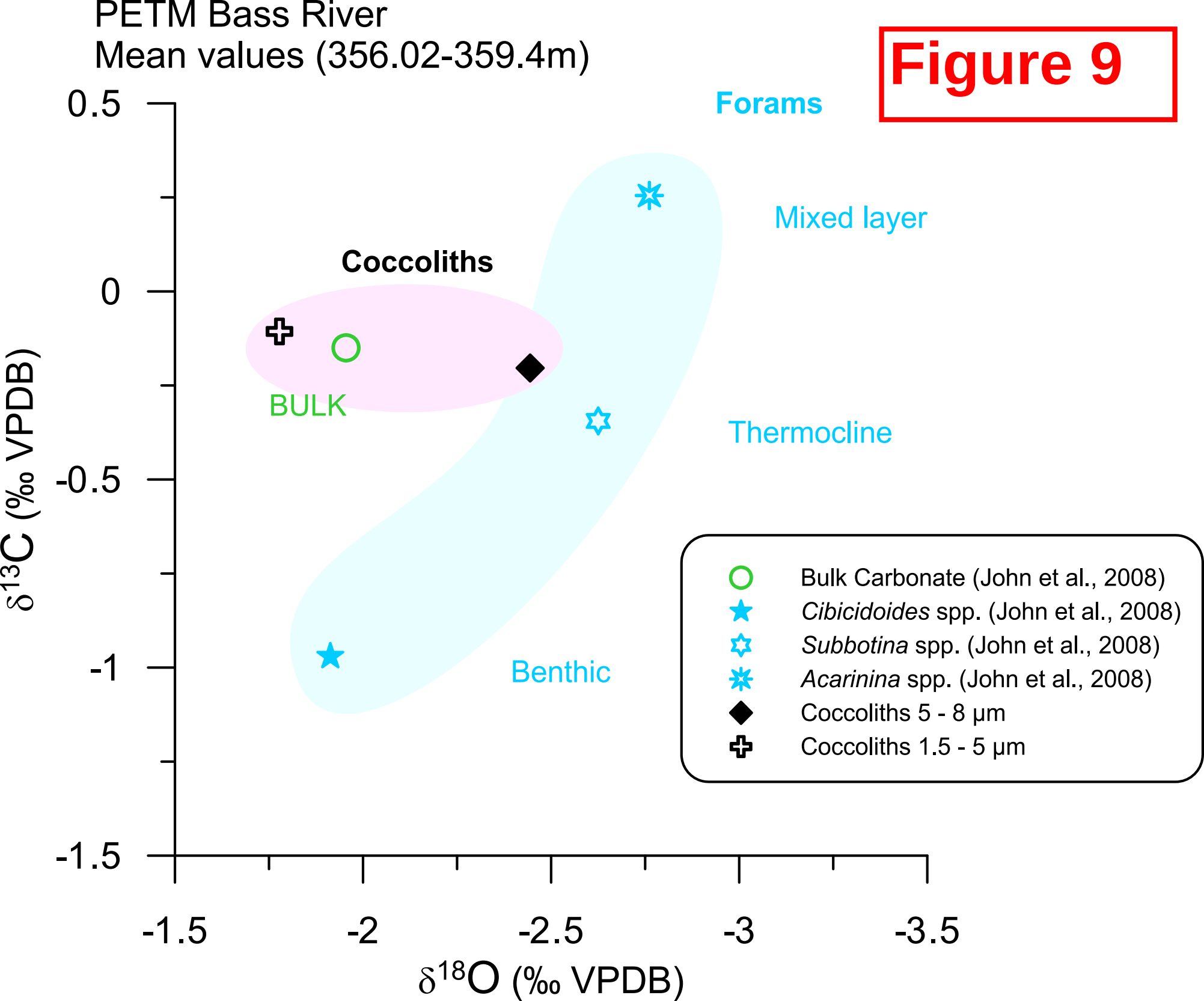
PETM Bass River
Mean values (356.02-359.4m)
Figure 9
Forams
Mixed layer
Coccoliths
BULK
Thermocline
Benthic
Bulk Carbonate (John et al., 2008)
Cibicidoides spp. (John et al., 2008)
Subbotina spp. (John et al., 2008)
Acarinina spp. (John et al., 2008)
Coccoliths 5 - 8 µm
Coccoliths 1.5 - 5 µm
0.5
0
-0.5
-1
-1.5
δ13C (‰ VPDB)
-1.5
-2
-2.5
-3
-3.5
δ18O (‰ VPDB)